A Survey of Venus Shock Crossings Dominated by Kinematic Relaxation

Simon Alexander Pope[1]

[1]University of Sheffield

November 21, 2022

Abstract

Collisionless shocks are one of the most effective particle accelerators in the known Universe. Even low Mach number shocks could have a significant role in particle heating and acceleration. Theory suggests that kinematic collisionless relaxation, the process whereby a downstream nongyroptopic ion population becomes thermalized through collisionless gyrophase mixing, is the dominant energy redistribution mechanism in quasi-perpendicular, low Mach number and low shocks. However, there have only been a limited number of observations of these shocks using in situ measurements at Venus, Earth and in inter-planetary space. This paper presents the results of the first detailed study using in situ measurements, of the effect of fundamental parameters on the formation of these shocks. All low Mach number shocks occurring during the magnetic cloud phase of an interplanetary coronal mass ejection are identified in Venus Express magnetic field data over the duration of the mission. From the 92 shock crossings identified, 38 show clear evidence of kinematic relaxation. It is shown that kinematic relaxation is dominant at Venus when the angle between the local shock normal and upstream magnetic field is greater 50° and the Alfvén Mach number is less than 1.4. These shocks are also observed across a range of solar-zenith-angles indicating that it is likely that any location on the Venus bow shock could form such a structure. Venus Express plasma measurements are used to verify the parameters estimated from the magnetic field and indicate the importance of heavy ions, including pickup O.

A Survey of Venus Shock Crossings Dominated by Kinematic Relaxation

S. A. Pope[1]

[1]Department of Automatic Control and Systems Engineering, University of Sheffield, Sheffield, UK

Key Points:

- First detailed study using in-situ measurements of the effect of fundamental parameters on kinematic relaxation at low Mach number shocks.
- Dependence of kinematic relaxation on the Aflvén Mach number and angle between the shock normal and upstream magnetic field are identified.
- A low Mach number bow shock with kinematic relaxation as the dominant energy re-distribution mechanism can form at most locations at Venus.

Corresponding author: Simon Pope, `s.a.pope@sheffield.ac.uk`

Abstract

Collisionless shocks are one of the most effective particle accelerators in the known Universe. Even low Mach number shocks could have a significant role in particle heating and acceleration. Theory suggests that kinematic collisionless relaxation, the process whereby a downstream nongyroptopic ion population becomes thermalized through collisionless gyrophase mixing, is the dominant energy redistribution mechanism in quasi-perpendicular, low Mach number and low β shocks. However, there have only been a limited number of observations of these shocks using in situ measurements at Venus, Earth and in inter-planetary space. This paper presents the results of the first detailed study using in situ measurements, of the effect of fundamental parameters on the formation of these shocks. All low Mach number shocks occurring during the magnetic cloud phase of an interplanetary coronal mass ejection are identified in Venus Express magnetic field data over the duration of the mission. From the 92 shock crossings identified, 38 show clear evidence of kinematic relaxation. It is shown that kinematic relaxation is dominant at Venus when the angle between the local shock normal and upstream magnetic field is greater 50°and the Alfvén Mach number is less than 1.4. These shocks are also observed across a range of solar-zenith-angles indicating that it is likely that any location on the Venus bow shock could form such a structure. Venus Express plasma measurements are used to verify the parameters estimated from the magnetic field and indicate the importance of heavy ions, including pickup O^+.

1 Introduction

Understanding collisionless shocks is important for many astrophysical processes. They are key providers of particle acceleration, both within the heliosphere and further afield. It is important to understand the physics of all types of collisionless shocks. Even low-Mach number shocks could have a significant role in particle acceleration and heating (Ryu, Kang, Hallman, & Jones, 2003). Within the heliosphere they have a key role in planetary interaction with the solar wind (Russell, 1985) and it is only here that they can be directly observed using in situ measurements. These direct observations therefore have important consequences for understanding astrophysical collisionless shocks. Their study within the heliosphere using direct observation, is also crucially important for many remote astrophysical objects, as radiation generated at collisionless shocks often provides the only observational data about the environment in the vicinity of these objects.

In a collisionless plasma a shock forms when a magnetosonic flow encounters an object and is subsequently decelerated to a sub-magnetosonic speed. When the flow is decelerated across the shock the upstream kinetic energy is re-distributed through various processes into thermalization of the bulk of the plasma flow and acceleration to high energies of a fraction of the particles. The processes that lead to this energy re-distribution vary depending on the shock parameters, most importantly the Mach number, the ratio of the upstream plasma kinetic to magnetic pressure (β) and the angle between the upstream magnetic field and normal to the shock surface ($\theta_{B,n}$). Understanding the role of the different processes that lead to the energy re-distribution is one of the most important tasks in collisionless shock physics.

One sub-set of shocks is those where the shock is quasi-perpendicular (i.e. $\theta_{B,n} \gtrsim 45°$). These shocks usually have a well structured magnetic field profile (Burgess, Wilkinson, & Schwartz, 1989; Kennel, Edmiston, & Hada, 1985; Mellott, 1985; Scudder et al., 1986). As the Mach number increase the magnetic field compression across the shock increases. The number of ions which are reflected and appear ahead of the shock ramp also increases and these have a significant effect on the structure of the shock (e.g. Scudder et al., 1986). The shock ramp can be defined as the region in the shock transition which has the steepest increase in the magnetic field. After crossing the shock ramp, the initially reflected ions form a superthermal population in the downstream region. The thermalization is a result of the combined gyration of the directly transmitted and initially reflected ions. In high Mach number supercritical shocks the reflected ions play a significant role in forming the downstream structure. In contrast, at low Mach number subcritical shocks the role of reflected ions is not considered to be significant. Instead, anomalous wave particle interaction was considered to be the main mechanism through which the kinetic energy was converted into heating in the downstream region for such shocks.

Under the accepted theory of low Mach number quasi-perpendicular shocks the magnetic field transition across the shock is smooth and ends in the downstream region without an overshoot or downstream oscillations (Kennel et al., 1985; Mellott, 1985). This is the case for both resistive and dispersive shocks. In contradiction to this accepted theory, Balikhin, Zhang, Gedalin, Ganushkina, and Pope (2008) observed low Mach number quasi-perpendicular shock crossings detected in the Venus Express magnetic field data, that had a noticeable overshoot and/or a significant downstream oscillations. They proposed that the source of this overshoot/oscillations was the kinematic relaxation of downstream ions with a non-gyrotropic velocity distribution. This was supported by theory and numerical analysis based on earlier work for downstream gyrating ion populations (Gedalin, 1996, 1997; Zilbersher, Gedalin, Newbury, & Russell, 1998). Balikhin et al. (2008) referred to such shocks as "kinematic shocks" in much the same manner as dispersive or resistive shocks are named after the predominant energy re-distribution process. The non-gyrotropy of the downstream ion distributions leads to a spatially dependent ion pressure, which due to the requirement for pressure balance, creates a spatially dependent and out-of-phase magnetic pressure (Gedalin, 2015). This is the cause for the overshoot and oscillations in the magnetic field observed by Balikhin et al. (2008). If the upstream ions have a non-cold distribution, spatial gyrophase mixing in the downstream regions leads to mixing of the plasma and consequently a decay in the magnitude of the oscillations. The rate of mixing is related to β. When β is low the relaxation length is large, so that a set of well-defined coherent oscillations can appear downstream of low Mach number shocks (Gedalin, 2015; Gedalin, Friedman, & Balikhin, 2015). The mixing of the directly transmitted and initially reflected ions at high Mach number shocks usually leads to significantly different downstream structure, often devoid of coherent oscillations (Gedalin, 2016; Ofman & Gedalin, 2013). Since the influence of reflected ions is expected to be small, low Mach number and low β shocks provide the best opportunity to observe and study the process of kinematic relaxation. This was confirmed by theoretical analysis and hybrid simulations conducted by Ofman, Balikhin, Russell, and Gedalin (2009).

Since this initial discovery by Balikhin et al. (2008), several other studies have focused on such shocks. This includes observation of low Mach number interplanetary shocks with such a structure in the magnetic field (Kajdič et al., 2012; Russell, Jian, Blanco-Cano, & Luhmann, 2009). Non-simultaneous magnetic field and plasma data was used to investigate interplanetary shocks with this structure (Goncharov et al., 2014). However, this did not directly confirm the anti-phase oscillations in the magnetic and ion pressure predicted by theory. Recently Pope, Gedalin, and Balikhin (2019) used the first observations of such shocks at the Earth to confirm this theory with direct simultaneous measurement of anti-phase oscillations in the magnetic and ion pressure. This study confirmed kinematic relaxation as the dominant process for energy re-distribution in these quasi-perpendicular low mach number shocks. It also showed the role of the different ion species (proton and α-particles in this case) in forming the downstream distribution.

Despite recent work, little is understood about the exact range of upstream conditions under which shocks dominant by kinematic relaxation form. Pope et al. (2019)

confirmed the most likely opportunity to observe such shocks at planets is during the magnetic cloud phase of an interplanetary coronal mass ejection (ICME). The magnetic cloud embedded within an ICME has the low Mach number and β environment predicted by theory as the most likely conditions under which kinematic relaxation can be observed. In addition, such shocks usually form at high altitude instances of the planetary bow shock, caused by the low Mach number solar wind. Zhang, Pope, et al. (2008) analyzed the location of the Venus bow shock during the planets interaction with a strong ICME. These shocks included those studied by Balikhin et al. (2008) and occurred at a much higher altitude than the nominal value determined using data from a similar time period (Zhang, Delva, et al., 2008). Suitable Earth observation satellites do not regularly explore such comparatively high altitudes. In contrast, extra-terrestrial inner-planetary exploration spacecraft, such as Venus Express, often have a much higher apoapsis and short orbital duration allowing this region to be sampled regularly and thus increasing the likelihood of observing such shocks when the solar wins conditions are suitable. In this paper the magnetic clouds identified by Vech et al. (2015) over the duration of the Venus Express mission are used as the search space for low Mach number shocks which show evidence of an overshoot and/or downstream oscillations. This paper identifies all instances of such shocks during these intervals. Following identification of these shocks, their structure are analyzed in terms of their dependence on key parameters such as Alfvén Mach number (M_A) and $\theta_{B,n}$. Their location in terms of solar zenith angle (SZA) and altitude are also investigated to determine if there is any bias for these shocks to form in a more sub-solar or flank location. The results show a clear range of upstream conditions under which these shocks occur. They also show that they can occur from the sub-solar through to flank locations at Venus.

2 Data

In this study magnetic field and plasma data measured by the MAG (Zhang et al., 2007) and ASPERA (Barabash, Sauvaud, et al., 2007) instruments onboard Venus Express was used. The primary data set is the 1Hz magnetic field measurements, which provides complete orbital coverage apart from during occasional planned or unplanned spacecraft operations. Using this data the initial search space for each planet was reduced by only considering the time periods when each planet was subject to an ICME with a clear and strong magnetic cloud. Previous studies have shown that these provide the most favorable conditions for observation of kinematic relaxation (Balikhin et al., 2008; Pope et al., 2019). The time intervals when Venus experiences the clear magnetic cloud phase of an ICME during the orbital mission lifetime of Venus Express (2006-2014) has previously been identified by Vech et al. (2015). This study identified six such intervals and these are investigated for the presence of shocks showing evidence of kinematic relaxation. This approach does not necessarily lead to the identification of all such shocks at Venus observed by Venus Express, but it should identify the majority and greatly speeds up the process of identification. Within these intervals, shock crossings were searched for which had: (1) Low magnetic compression (B_d/B_u across the shock ($\lessapprox$ 1.5), indicative of a very low Mach number; (2) Low-frequency downstream oscillations polarized along the shock normal direction which onset immediately after the shock ramp; and (3) Multiple crossings of this shock structure. Criteria number 3 isn't strictly required as initial evidence of observation of a shock dominated by kinematic relaxation, but it can aid in their identification. The reason is that the Venus bow shock altitude is primarily driven by the solar wind Mach number (Russell et al., 1988). Since the shocks of interest occur during very low Mach numbers, even small changes can lead to significant changes in bow shock location. In-particular, in a very low Mach number magnetic cloud the proton density is usually very small. For example, it is close to unity for the kinematic shock observed at the Earth (Pope et al., 2019). In this case even a small absolute change in proton density can lead to a significant relative change in M_A. Multiple bow shock crossings by Venus Express due to a dynamic bow shock moving back and forth across the slower moving spacecraft, are therefore often a signature of the very low Mach number conditions of interest. Following identification of the shocks in the magnetic field data, ASPERA proton number density, temperature and velocity and Oxygen number density at 192s sample intervals with good/excellent quality flags was used to further study the upstream conditions. The plasma data does not provide complete orbital coverage, so data was not available for all shock crossings identified.

Due to the reliance on single spacecraft measurements with low-sample rate and non-continuous plasma measurements, the shock normal $\hat{\mathbf{n}}$ for each of the shocks studied, is determined from the magnetic field data using both minimum variance analysis (MVA) and the coplanarity theorem (CP). Both of these methods can be subject to errors due to factors such as a small number of data samples across the shock ramp and the presence of non shock related structures in then upstream and downstream regions. However, if carefully implemented they can be used to determine a reasonably accurate estimate of the shock normal. As an example, in Pope et al. (2019) there was $< 4°$ between the MVA and CP normal and that calculated using the double coplanarity theorem which requires both the magnetic field and ion velocity data. Due to the often abnormally high altitude of the observed shocks, the shock normal calculated using a model bow shock and observed SZA (solar zenith angle) was not considered. The shock normal is used to determine the angle between the average upstream magnetic field and shock normal direction $\theta_{B,n}$.

When suitable plasma data was available the Alfvén Mach number was calculated directly as $M_A = v_{u,x}/v_A$, the ratio of the upstream flow velocity $v_{u,x}$ in the shock normal direction in the shock rest frame, to the upstream Alfvén speed $v_A = B_u^2/\mu n_{i,u} m_i$ (B_u is the average upstream magnetic field magnitude, $n_{i,u}$ is the upstream ion density and m_i is the ion mass). In the calculation of the Alfvén velocity the subscript i is the ion species. Where possible, single (proton) and multi-fluid (proton and Oxygen) v_A were calculated and the importance of including heavy ions investigated. The Alfvén Mach number for all of the detected very weak shocks was estimated directly from the magnetic field data using $M_{A,B} \approx \sqrt{R\,(R+1)\,/2}$, where $R = B_d/B_u$ is the ratio of the downstream and upstream magnetic field magnitudes. This is valid for a cold perpendicular shock (Gedalin et al., 2015). Pope et al. (2019) recently showed good agreement between this estimate and the directly calculated value of M_A for the very-low Mach number shock in which kinematic relaxation dominates, which was observed at the Earth. The Magnetosonic Mach number wasn't considered, since in an ICME magnetic cloud the Alfvén speed is usually significantly larger than the sound speed. This is caused by the abnormally large (for the solar wind) magnetic field and the low proton temperature and often low proton densities (L. Burlaga, Sittler, Mariani, & Schwenn, 1981; Leamon, 2002)

The upstream $\beta_{i,u} = p_i/p_B = 2\mu_0 p_u/B_u^2$ (the ratio of kinetic to magnetic pressure), is calculated when suitable plasma data is available. The total kinetic pressure in the solar wind is estimated using the available proton density and temperature data as $p_u = n_{p,u} k_b (1.16 T_{p,u} + 1.55 \times 10^5)$ (L. F. Burlaga & Ogilvie, 1970). Finally, the SZA and altitude A of the observed shocks are determined. These are compared to model shock altitudes A_m at solar minimum for the observed SZA (Zhang, Delva, et al., 2008), i.e. when the bow shock is on average at its most compressed.

3 Observations

Six intervals during which Venus Express observes the magnetic cloud phase of an ICME, as identified by Vech et al. (2015), are shown in Figure 1a-f. For each of these six intervals, Venus Express observes at least one group of multiple crossings of very-low Mach number shock. These groups of shock crossings are marked by the colored regions in Figure 1a-f. The profile of the magnetic field magnitude and the shock parameters (mainly derived from the magnetic field measurements) for all of these shock crossings on each of these six days, are contain in the supplementary information in Figures S1-S6 and Table S1-S6 respectively. A subset of these which show certain interesting characteristics, or for which plasma data is available, are included in Figures 2-4 and Table 1 and discussed in the following subsections.

3.1 10th-11th September 2006

The shocks previously studied by Balikhin et al. (2008) occurred on 10th September 2006 during an ICME with a prolonged magnetic cloud, which commenced at around 18:20 UT on 10th September and continued throughout the following day, spanning an entire Venus Express orbit. The magnetic field measured by Venus Express during this period is shown in Figure 1a. The red shaded region marks the seven shock crossings which were studied by Balikhin et al. (2008) and occurred on the inbound trajectory of Venus Express, but at an abnormally high altitude. The spacecraft then detects two more sets of shocking crossings on the outbound and the the next inbound trajectory. These are marked by the green and blue regions in Figure 1a. Figure S1 shows the profile in the magnetic field data and Table S1 contains the magnetic field derived parameters for all of these individual shock crossings.

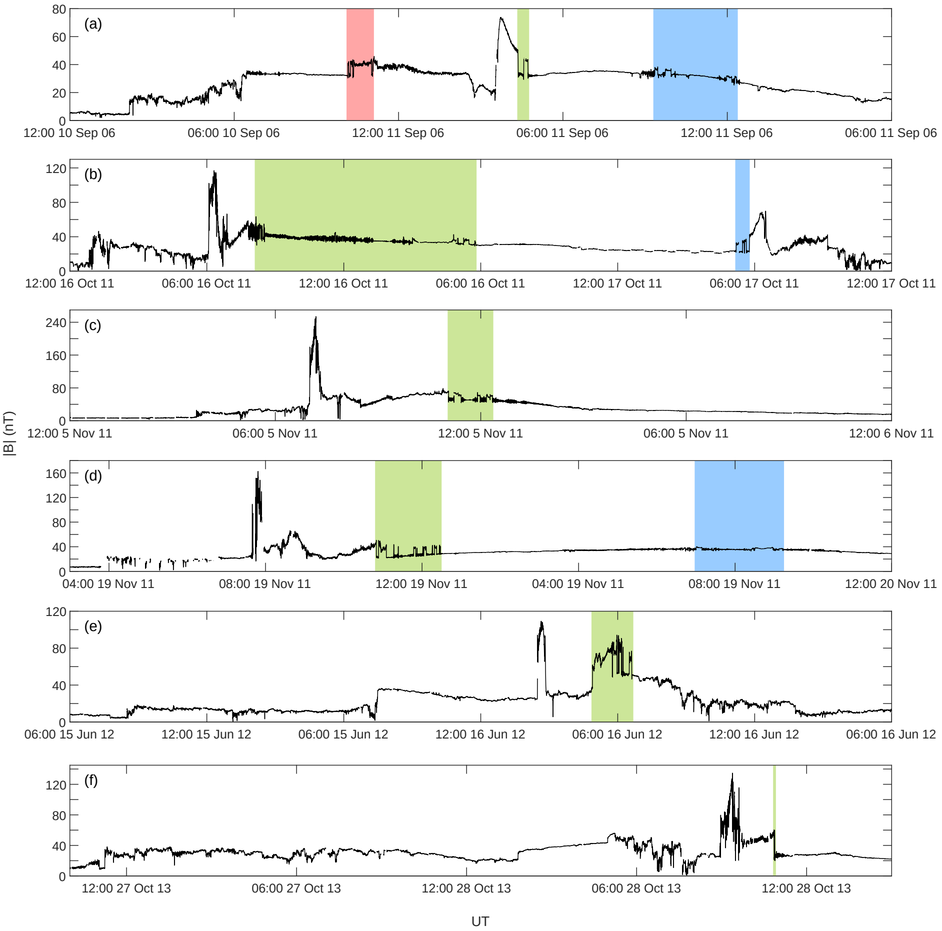

Figure 1. Venus Express magnetic field magnitude plotted for six different intervals in panels (a)-(f). The red shaded region in panel (a) indicates the original group of shocks studied by Balikhin et al. (2008). The green and blue shaded regions in panels (a)-(f) indicate new groups of very-low Mach number shocks identified in this study. For clarity of presentation, the limits of both the time and magnetic field axes are set independently for each panel (a)-(f).

Table 1. Magnetic field derived parameters for five separate groups of Venus bow shock crossings detected in Venus Express data on three separate days. ND indicates no data due to a gap in the measurements.

Shock	$\theta_{B,n_{mv}}$ (°)	$\theta_{B,n_{cp}}$ (°)	$M_{A,B}$	SZA (°)	A (R_V)	A_m (R_V)
10th-11th September 2006						
2a	72	71	1.37	40	2.78	1.45
2b	72	76	1.27	45	3.27	1.49
2c	75	51	1.24	49	3.63	1.52
3a	70	49	1.07	81	9.72	1.95
3b	85	63	1.07	82	9.80	1.97
3c	68	64	1.07	82	10.00	1.97
3d	77	53	1.09	83	10.20	1.99
3e	54	47	1.06	88	11.30	2.09
3f	74	54	1.07	89	11.30	2.12
3g	58	55	1.07	89	11.40	2.12
3h	64	64	1.06	89	11.40	2.12
16th-17th October 2011						
1a	30	26	1.18	123	4.77	3.23
1b	30	21	1.17	123	4.81	3.23
1c	45	52	1.11	108	9.21	2.65
1d	50	42	1.17	108	9.25	2.65
1e	63	63	1.11	101	11.17	2.43
1f	65	67	1.11	101	11.18	2.43
1g	86	62	1.11	101	11.34	2.43
1h	77	58	1.08	97	11.87	2.32
1i	83	42	1.12	97	11.88	2.32
1j	84	70	1.12	97	11.89	2.32
1k	78	43	1.09	97	11.92	2.32
1l	80	64	1.11	96	11.95	2.29
1m	80	66	1.09	96	11.97	2.29
1n	57	11	1.05	96	11.98	2.29
2a	72	71	1.24	59	3.90	1.62
2b	76	68	1.33	58	3.68	1.61
2c	66	65	1.37	55	3.29	1.58
2d	81	72	1.37	54	3.11	1.57
2e	67	68	1.40	54	3.08	1.57
2f	75	68	1.36	52	2.90	1.55
2g	74	69	1.56	50	2.57	1.53
19th November 2011						
2a	48	41	1.05	101	11.97	2.43
2b	77	55	1.06	101	11.98	2.43
2c	60	39	1.03	98	11.99	2.34
2d	45	33	1.06	96	11.95	2.29
2e	35	2	1.01	96	11.93	2.29
2f	46	20	1.02	96	11.92	2.29

Figure 2 shows the three shock crossings in the second group and eight shock crossings in the third group (i.e. the green and blue shaded regions in Figure 1a). Table 1 contains the associated shock parameters mainly derived from the magnetic field data. All of the shocks in the second group are quasi-perpendicular with $\theta_{B,n} = 72 - 75°$. This is based on the MVA derived shock normals as they give consistent values across the three closely spaced shock crossings. When there are no data gaps present all three shock crossings show a structure with an overshoot and downstream oscillations of varying magnitude. They also all have a very-low Alfvén Mach number, estimated to be in the range 1.24-1.37. The range of Mach numbers and $\theta_{B,n}$ for these shock crossings is very similar to the shock crossings previously studied by Balikhin et al. (2008), i.e. the first group of shock crossings ($\theta_{B,n} = 76{-}87°$ and $M_A = 1.19{-}1.23$). They are also very similar to the very-low Mach number shocks dominated by kinematic relaxation that were recently reported at the Earth by Pope et al. (2019). All of the shock crossings in the third group (blue region) are also quasi-perpendicular, but with values closer to 45° and even lower Alfvén Mach number in the range 1.06-1.09. All of these shocks, apart from shock 3f, also show a structure with an overshoot and downstream oscillations of varying magnitude. These two additional groups of shock crossings (apart from 3f) on 11th September 2006, can be categorized as being very-low Mach number shocks dominated by kinematic relaxation. The original group of shocks investigated by Balikhin et al. (2008) occurred on the nightside flank (SZA = 112-116°) and at abnormally high altitude of 8.6-9.4 R_V, compared to a model value of 2.79-2.94 R_V at solar minimum. In contrast the second group of shocks extends observations to the dayside (SZA = 40-49°) and as a consequence a much lower altitude (2.78-3.63 R_V). This is still much higher than the nominal bow shock location of 1.44-1.52 R_V. The third group of shocks covers the dayside terminator region (81-89°) and very high altitude of 9.72-11.4 R_V. This is 5.0 to 5.4 times greater than the nominal bow shock altitude.

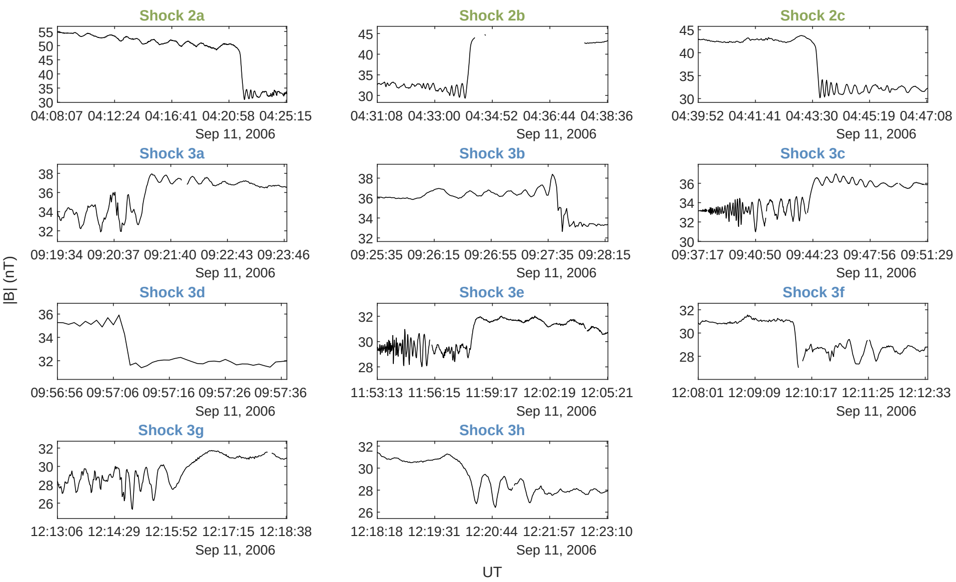

Figure 2. Venus Express magnetic field magnitude plotted for separate intervals showing the individual shock crossings identified for group 2 and 3 on 10th-11th September 2006, i.e. each of the shock crossings in the green and blue shaded regions highlighted in Figure 1a. The shocks are labeled 2a-2c and 3a-3h. For clarity of presentation the limits of both the time and magnetic field axes are set independently for each panel.

No suitable plasma data was available for the original group of shock crossings studied by Balikhin et al. (2008). However, for both of the second and third group of shock crossings, plasma data is available. This can be used to help verify the parameters derived from the magnetic field data and also provide additional insight. For the second group of shocks, ASPERA plasma data is available for the duration of the required period. The quality flag of this data is only excellent for the first shock crossing in the sequence and falls to satisfactory for the subsequent two crossings. This is sufficient to determine the upstream conditions between the first two shocks. Due to the low density and temperature and high magnetic field magnitude when compared to nominal solar wind conditions at 0.72AU, β is very-low (0.02-0.03) and the proton only Alfvén velocity is high (457 km/s). The upstream parameters used to calculate these values are given in Table S7. Calculating the proton only Alfvén Mach number using the minimum variance shock normal and assuming a shock velocity of zero, leads to $M_A = 0.74$ for the first shock. The assumption of zero shock velocity is incorrect, since for the shock to pass back and forth across the spacecraft over a short period of time requires a non-zero shock velocity. However, this value of M_A is not particularly sensitive to assuming a shock velocity of zero. For example, a shock velocity of 20km/s directed outwards (away from Venus) gives only a marginally higher $M_A = 0.78$. The value of $M_A < 1$ could be due to measurement errors associated with the low number density. Considering the excellent data flag, another reason could be a significant heavy ion component, which can act to lower the Alfvén velocity. Pope et al. (2019) have previously shown the contribution that a heavy ion component in the solar wind in the form of α-particles, can play for kinematic shocks. At Venus it is well-known that pickup ions can be abundant, in-particular O^+ (e.g. Barabash, Fedorov, et al., 2007; Fedorov et al., 2011). The plasma data does not indicate a significant heavy ion component, but an O^+ number density of 15% that of the protons, would sufficiently lower the Alfvén velocity to give the required $M_A = 1.37$ estimated for the first shock using the magnetic field.

For the third group of shock crossings (blue shaded region), the plasma data is available for a short time interval approximately 3 hours after the last crossing. Vech et al. (2015) previously calculated the magnetosonic Mach number for this magnetic cloud as 1.12. It is unclear which interval of plasma data was used to determine this value. Using the proton and magnetic field data measured 3 hours after the last shock, gives $M_A = 1.41$. The upstream parameters used to calculate this value are given in Table S7. Alternatively, using the same proton data but the higher magnetic field magnitude at the shock crossing locations, gives $M_A = 1.03$. This is consistent with the Alfvén Mach numbers of 1.06-1.09 estimated for these distant shocks using the magnetic field data. The calculation of $M_A = 1.03$ at the shock location assumes that the proton velocity and density is comparable to that measured 3 hours later and does not take into account the normal incidence frame transformation. However, it does provide an indication of the very-low Mach number nature of the magnetic cloud around the time of these shocks. The value of β is 0.08 if the plasma data measured 3 hours after the third group is used. It falls to 0.04 if the magnetic field data at the last crossing in the third group is used. The values of β calculated for both groups is consistent with the assumption of a very-low β and with $\beta < 0.1$ during the shock observations at the Earth (Pope et al., 2019).

3.2 16th-17th October 2011

Another prolonged magnetic cloud occurred during an ICME that arrived at Venus on 16th October 2011. The magnetic cloud commenced at some point while Venus Express was within the induced magnetosphere of Venus. The spacecraft subsequently detected a group of thirteen shocking crossings on its outbound and then seven shock crossings on its inbound trajectory during the magnetic cloud. The first group occurred on the flank (SZA 96-123°). All of these shock crossings exhibit a very-low magnetic compression and are marked by the green shaded region in Figure 1b. The second group occurred on the day side and are marked by the blue shaded region in Figure 1b. All of the shock crossings in the second group have a very-low magnetic compression and downstream oscillations of varying magnitude. The important magnetic field derived parameters for these shocks are shown in Table 1 and their magnetic profiles are shown in more detail in Figure 3.

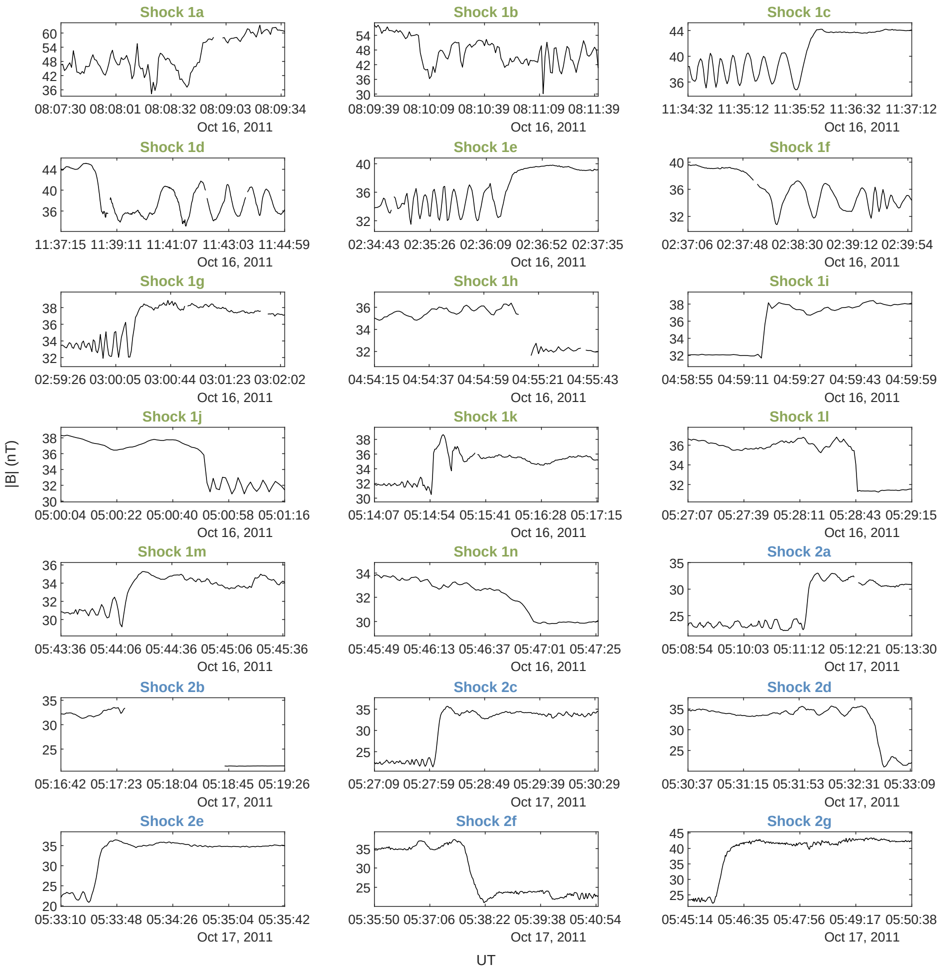

Figure 3. Venus Express magnetic field magnitude plotted for separate intervals showing the individual shock crossings identified for group 1 and 2 on 16th-17th October 2011, i.e. each of the shock crossings in the green and blue shaded regions highlighted in Figure 1b. The shocks are labeled 1a-1n and 2a-2g. For clarity of presentation the limits of both the time and magnetic field axes are set independently for each panel.

The first group of shock crossings start on the night side flank at an altitude slightly above the model altitude and progress to close to the terminator at an altitude much higher (just over five times higher) than the model value. The earlier crossings in the sequence start off as quasi-parallel shocks, with both the minimum variance and coplanarity normal agreeing reasonably well and proceed to become quasi-perpendicular shocks. The minimum variance and coplanarity normal don't agree as well later in the sequence, with the most likely reason the presence of numerous local rotations in the solar wind magnetic field. The transition from quasi-parallel to quasi-perpendicular shock is consistent with the observed slow rotation of the field in the magnetic cloud over this interval. Only crossing 1j, l and m are definitively quasi-perpendicular (both shock normal's are $> 60°$) and have a sufficiently long period in the downstream region to observe the presence of oscillations due to kinematic relaxation. The most interesting shock crossings in terms of observation of kinematic relaxation are those in group 2. These consist of seven closely spaced shock crossings much closer to the sub-solar point. They occurred at SZA 50-60°and at an altitude 1.7-2.4 times higher than the model altitude. This further adds to the SZA at which this type of shock has been observed. All of these shock crossings are well defined as quasi-perpendicular and with generally good agreement between the two shock normal directions. The coplanarity normal in-particular doesn't deviate much across all seven crossings. As the planet is approached the estimated Mach number gradually increases from 1.24 to 1.56, as would be expected for a more compressed induced magnetosphere. All of these shock crossings have well defined downstream oscillations, apart from crossing 2b which has a data gap across the ramp and into the downstream region. The absolute magnitude of the downstream oscillations is approximately the same for all of these shock crossings ($2.2 \pm 0.6nT$), but relative to the size of the shock ramp their magnitude decreases from 0.3 to 0.1.

For the first group there is no simultaneous plasma data. However, with the second group there is simultaneous plasma and magnetic field measurements. This allows the upstream conditions to be resolved. Within this second group there are two longer solar wind intervals with excellent quality flag (the time intervals between shock crossing 2b and 2c and crossing 2f and 2g). The plasma data upstream of shock 2a is not used due to the lower quality flag and the interval between 2d and 2e is too short compared to the sample time of the plasma data to extract any meaningful measurements. These plasma data intervals are used together with the simultaneous upstream magnetic field averages for shock crossing 2c, 2f and 2g to calculated some of the important shock parameters. Shock crossing 2b is not considered due to the data gap. The upstream parameters used to calculate the values are given in Table S8.

All three shocks are low β with values of 0.08 for shock 2c and 0.1 for shock 2f and 2g. The Alfvén Mach numbers are calculated using a shock velocity of 0 km/s and the coplanarity shock normals. This gives values of 1.28, 1.22 and 1.44 for shock crossing 2c, 2f and 2g respectively, which is 7, 11 and 9% smaller than the Mach numbers estimated using the magnetic field. The spacecraft velocity projected onto the shock normal is 3-5 km/s, indicating that a relatively small shock velocity would be required to create the oscillatory back and forth motion across the spacecraft trajectory. Including a shock velocity of $\pm 20km/s$ leads to a small 4-6 % change in the estimated Mach number, indicating that other factors might also contribute to the difference. Other than uncertainties in the measurements used and the contribution from the shock velocity, another reason for this difference would be the presence of heavy ions. The Venus Express plasma data indicates a very small and fluctuating component of O^+ ($< 3\%$ by number compared to the proton density). Taking into account 1-2% O^+ increases the Alfvén Mach numbers to the values of 1.37, 1.36 and 1.56 estimated from the magnetic field. This indicates the sensitivity of very low Mach number calculations to the presence of even a small amount of heavy ions and the role that they might play.

3.3 5th November 2011

On the 5th November 2011 Venus interacts with an ICME that leads to the detection of a bow shock with a large magnetic compression of 3.44 on the inbound trajectory of Venus Express. This strong shock and associated effect of the ICME on the Venus interaction region has been studied by Dimmock et al. (2018) using a combination of observations and hybrid simulations. Within the ICME a large magnetic cloud with a peak measured magnetic field of 50nT commences at some point while the spacecraft is in the magnetosheath or induced magnetosphere and continues until the end of the day. During the magnetic cloud phase Venus Express crosses the bow shock seven times at SZA 123-117° and altitude 7.79-9.11 R_V. These shock crossings are marked by the green shaded region in Figure 1c. Figure S3 shows the profile in the magnetic field data and Table S3 contains the magnetic field derived parameters for the individual shock crossings. All of these shock crossings have a low magnetic compression leading to estimated Alfvén Mach numbers of 1.15-1.26. The altitude of all of the shock crossings are considerably above the model altitude at the respective SZA, with a tendency for this difference to increase as the Mach number reduces. All of the shock normals derived by the coplanarity theorem lie within 40° (60% lie within 20°) of each other. However, despite this reasonably good agreement, $\theta_{B,n}$ ranges between 11 and 67° due to numerous short and long interval rotations in the magnetic field during the magnetic cloud. Three of these shocks have $\theta_{B,n} \geq 50°$ and two of these (1a and 1d) show clear evidence of an overshoot and downstream oscillations of varying magnitude. No plasma data is present at or near the interval in which these crossings occur.

3.4 19th November 2011

On 19th November 2011 Venus interacts with an ICME which reaches Venus while Venus Express is in the solar wind. The magnetic cloud phase commences shortly before the spacecraft crosses the Venus bow shock on its inbound trajectory and continues until the end of the day. The spacecraft detects a sequence of 23 shock crossings associated with a very dynamic shock motion over an interval of 1 hour and 40 minutes on its outbound trajectory. These shock crossings (shock group 1) are indicated by the green shaded region in Figure 1d. Figure S4 shows the profile in the magnetic field data and Table S4 contains the magnetic field derived parameters for the individual shock crossings. These crossings occur from SZA 130-121° and at an altitude of 6.75-8.67R_V. The magnetic compression gradually drops across the interval, such that the estimated Alfvén Mach number falls from 1.7 to 1.3. All of the shocks are quasi-perpendicular for both shock normal calculations with $\theta_{B,n}$ ranging from 61-81° (average of the two values for each shock crossing). The shock crossings have a tendency to become more perpendicular through the interval. When the downstream interval for each crossing is sufficiently long to allow this region to be investigated, clear downstream oscillations only become evident later in the sequence from shock 1n onwards. No plasma data with good/excellent quality flags is available for this interval.

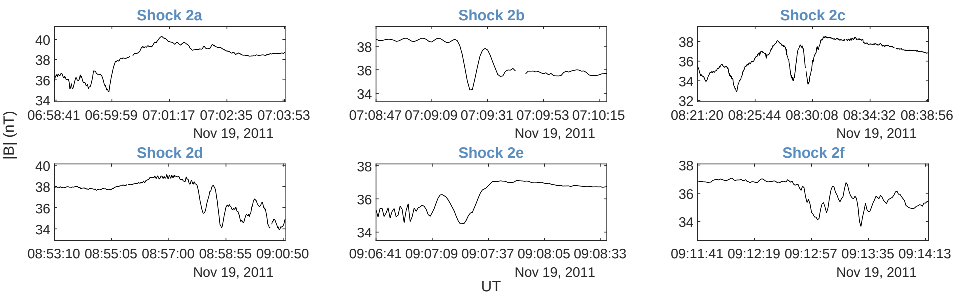

Figure 4. Venus Express magnetic field magnitude plotted for separate intervals showing the individual shock crossings identified for group 2 on 19th November 2011, i.e. each of the shock crossings in the blue shaded region highlighted in Figure 1d. The shocks are labeled 2a-2f. For clarity of presentation, the limits of both the time and magnetic field axes are set independently for each panel.

Venus Express subsequently encounters six additional shock crossings between 19:00 and 21:15 UT. These shock crossings (group 2) are indicated by the blue shaded region in Figure 1d. The important magnetic field derived parameters for these shocks are shown in Table 1 and their magnetic profiles are shown in more detail in Figure 4. They occur over an interval near the peak magnetic field in the cloud and from SZA 101-96°and altitude 11.97-11.92 R_V. The estimated Mach numbers of these shock crossings is very-low and in the range 1.01-1.06. To our knowledge these are the lowest Mach number shocks that have been observed at Venus. The altitude of all of the shock crossings on 19th November 2011 are considerably above the model altitude at the respective SZA, with a tendency for this difference to increase as the Mach number reduces. The ratio of observed to nominal model altitude for the lowest Mach number shocks in group 2 is just over five, which is consistent to the other days when the Mach number is just above 1. The shock normals indicate that they are all oblique to quasi-parallel with a tendency to become more parallel through the interval, apart from crossing 2b which is quasi-perpendicular. The change in shock normal for this shock crossing is due to a small rotation in the field in the downstream region just before the spacecraft crosses the shock back into the magnetic cloud. The quasi-perpendicular shock crossing 2b has $\theta_{B,n} = 66°$ (average of the two shock normal calculations) and an estimated Mach number of 1.06. It is also evident that the downstream region contains a clear sequence of oscillations, indicating the presence of kinematic relaxation. For the last three shock crossings in this sequence good/excellent quality proton data is available. Using the observed upstream proton measurements just after the last shock and taking into account 10% O^+ (the quality flag for O^+ fluctuates such that the number density varies significantly between 0 and approximately 80%) the Alfvén Mach number of the bulk flow is estimated as 1.01 and β as 0.04. These are only approximate values due to the low sample rate of the data and errors associated with determining such low and marginal values. However, they do serve as an indication of the very low Mach number and β nature of the magnetic cloud. The upstream parameters used to calculate these values are given in Table S9.

3.5 16th June 2012

On 15th June 2012 Venus Express detected the leading shock of an ICME while in the solar wind. The magnetic cloud phase commenced at about 19:30UT and continued into the following day. Venus Express detected 14 shock crossings on its outbound trajectory from SZA 137-125°and altitude 5.43-7.83 R_V. These shock crossings are indicated by the green shaded region in Figure 1e. Figure S5 shows the profile in the magnetic field data and Table S5 contains the magnetic field derived parameters for the individual shock crossings. All of these shocks are quasi-perpendicular with all but one $\theta_{B,n} = 72 - 84°$ (average values from the two shock normal calculations) and 60% have $\theta_{B,n} \geq 80$. The one exception (shock crossing 1j) has $\theta_{B,n} = 65°$. As such, these are the closest to "perpendicular" very-low Mach number shocks observed in this study. All of these shocks have a very-low estimated Mach number, which starts at 1.44 and 1.47 for the first two shocks and gradually falls through the interval to 1.24 for the last shock. The altitude of all of the shock crossings are above the model altitude at the respective SZA, with a tendency for this difference to increase as the Mach number reduces. Most of these shocks show evidence of downstream oscillations or an overshoot, but some show evidence of neither. However, the sampling interval is relatively long with respect to the time required to cross the shock ramp, which might inhibit the possibility of clearly observing any downstream oscillations. Plasma data is available for most of this interval, but excellent/good quality proton data is only available in the region upstream of the first shock. For this interval and using the upper limit of measured oxygen contribution of 4% by number (the oxygen data varies from bad to good in this region), $M_A = 1.45$ for the bulk solar wind flow. This Mach number agrees very well with 1.44 estimated from the magnetic compression of the first shock. The value of $\beta = 0.20$ is notably larger when compared to the shock crossings observed on the other days. The upstream parameters used to calculate these values are given in Table S10.

3.6 28th October 2013

On 27th October 2013, just before midday, Venus Express detects the leading shock of an ICME. The ICME continues into the 28th October and a magnetic cloud phase commences around the time that the spacecraft crosses the Venus bow shock on its inbound trajectory. The magnetic cloud phase continues until the end of the day, but the magnetic field gradually weakens to a magnitude representative of the undisturbed solar wind at 0.72AU. On the outbound trajectory, Venus Express encounters three closely spaced bow shock crossings at SZA 114 and altitude 4.20-4.26 R_V. These shock crossings are indicated by the green shaded region in Figure 1f. Figure S6 shows the profile in the magnetic field data and Table S6 contains the magnetic field derived parameters for the individual shock crossings. These crossings have a reasonably low magnetic compression leading to estimated Alfvén Mach numbers of 1.70-1.85. The altitude of all of the shock crossings are approximately 50% higher than the model altitude at the respective SZA. The shock normal determined for the three shock crossings using both methods agree reasonable well, such that $\theta_{B,n} = 53 - 62°$. This indicates that the shocks are quasi-perpendicular, but towards the lower end of the possible range of $\theta_{B,n}$. The spacecraft spent sufficient time in the downstream region of only the first crossing to detect a clear set of downstream oscillations. For this first shock crossing there is some indication of downstream oscillations, but they are of low magnitude and only last two to three wave periods. The magnetic field in the magnetic cloud is not particularly large at the time of the shock crossings. This would reduce the Alfvén velocity and raise β. Unfortunately the proton data that is available has low quality flags, preventing a direct calculation of these values.

4 Discussion

When plasma data is available for these shock crossings the calculated Alfvén Mach number is generally in good agreement with that estimated from the magnetic field data. This gives confidence in using the estimated Mach number for further analysis of these shocks. It also indicates that β, the ratio of kinetic to magnetic pressure, is low for these shocks. The calculated values are $\beta \leq 0.1$ for all but one value, which is $\beta = 0.2$. Figure 5 plots $\theta_{B,n}$ (average of the coplanarity and minimum variance derived values) against the estimated Alfvén Mach number. Each shock is plotted as a symbol which represents one of four conditions (downstream oscillations present, no downstream oscillations present, overshoot present and potential downstream oscillations, overshoot only). Figure 5 shows that only quasi-perpendicular very-low Mach number shocks show evidence of the downstream oscillations created by kinematic relaxation. Most of the shocks with evidence of downstream oscillations are clustered in the region defined by $\theta_{B,n} > 50°$ and $M_A < 1.4$. The transition from this region to more quasi-parallel and higher Mach numbers is indicated by the shocks with potentially some evidence of downstream oscillations, or with only an overshoot. The existence of these transition regions provides good evidence that kinematic relaxation is only clearly observable for very-low Mach number quasi-perpendicular shocks. Evidence of just an overshoot for these shocks is likely to be due to the formation of less than one period of downstream oscillations, i.e. a situation in which the oscillations are quickly damped. A higher damping rate for smaller values of $\theta_{B,n}$ would be consistent with theory (Gedalin, 2015). However, a longer wave train is expected for higher magnetic compression. The reason for the clear transition observed in Figure 5 could be that the upstream β is greater for these shocks. Since β cannot be consistently measured for all of the shocks in this study, it's effect on this transition cannot be verified.

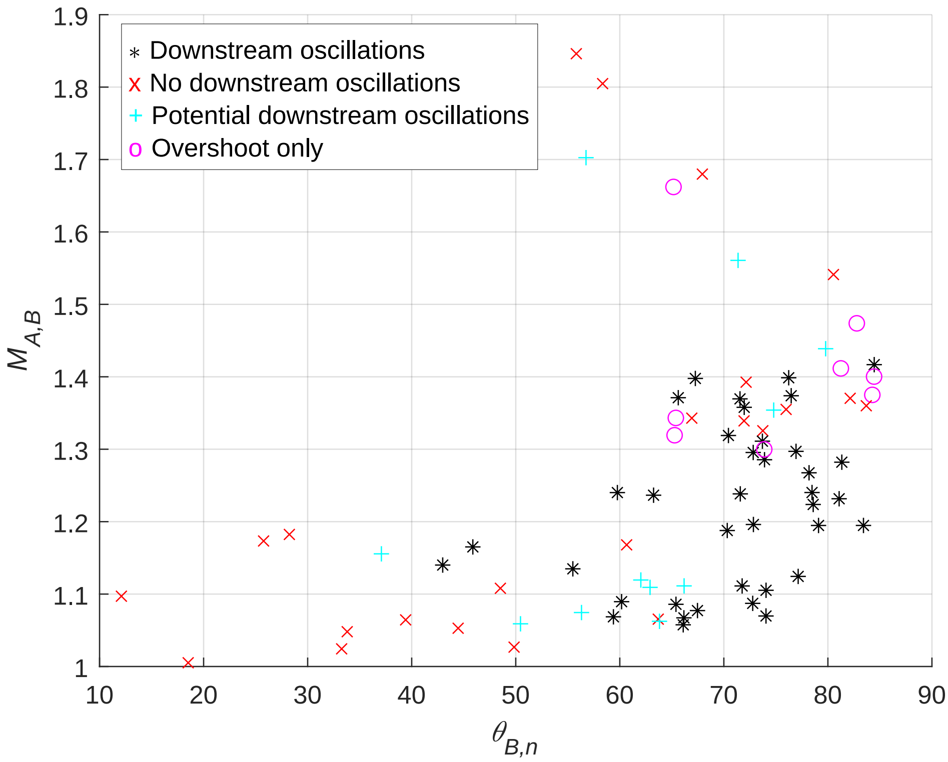

Figure 5. A plot of $\theta_{B,n}$ against M_A for all of the very-low Mach number shocks identified for the duration of the Venus Express mission. The presence of downstream oscillations or overshoot is indicated by the different colored symbols.

Additional evidence of this transition from lower to higher Mach numbers can be seen in some of the sequences of shock crossings on each of the days. All of the shock crossings in shock group 2 on 17th October 2011 are quasi-perpendicular with very similar $\theta_{B,n}$, but the Mach number increases throughout the sequence. As seen from Figure 3, both the magnitude of the oscillations with respect to the ramp magnitude and the number of observable periods of the oscillations decreases throughout the sequence. When it is available the plasma data indicates that β doesn't change significantly across these shocks (for shock 2c $\beta = 0.08$, shock 2f $\beta = 0.10$ and shock 2g $\beta = 0.10$). This indicates that the observed changes are due to the increase in Mach number and are not due to changes in β. A second example is shock group 2 on 19th November 2011. All of these shocks have a similar very low Mach number and all are quasi-parallel, apart from shock 2b. As seen from Figure 4, it is only the quasi-perpendicular shock 2b that has downstream oscillations present. The final example is shock group 3 on 10th September 2006. All of these shocks have a similar very-low Mach number, but $\theta_{B,n}$ becomes smaller through the sequence so that the final two shocks are close to the bottom limit of the region in which kinematic relaxation is observed in Figure 5. As seen from Figure 2, the early shocks have a clear and sustained set of downstream oscillations and as the sequence progresses the downstream oscillations become less prominent. This is consistent with a transition towards the lower limit of $\theta_{B,n}$ in which kinematic relaxation is observed.

When calculating the Alfvén Mach number from the plasma data it was found that the contribution from heavy ions in the form of O^+ needed to be included to get a match to the values estimated from the magnetic field data. Pope et al. (2019) showed the role of heavy ions in forming the downstream distribution. In the case of the Earth, α-particles in the magnetic cloud were the source of heavy ions. It was shown that they contribute to the pressure balance by providing both a fixed and oscillating component to the dynamic pressure. At Venus there will still be α-particles present in the magnetic cloud and likely of a similar amount to that investigated by Pope et al. (2019). However, pick-up ions are also likely to have a similar effect and ASPERA data does indicate a potentially significant population of O^+. Due to the dependence of the wavelength of these oscillations on the ion gyro-frequency, the observed period will be 1/16 that of the protons. Therefore, it is unlikely that such a long period will be observable in the data due to insufficient time spent in the downstream region. The largest number of oscillations observed due to protons is 9, i.e. approximately half the wavelength of the O^+ oscillations. The two most promising candidates for observation of oscillations due to O^+ are shock 3c during 10-11th September 2006 and shock 1n during 16th June 2012. Both of these shocks have 8-9 clear downstream oscillations which are superimposed onto a much slower change. The frequency of this slower change would be consistent with approximately 1/16 that of the higher frequency proton oscillations.

The very-low Mach number shocks identified in Venus Express data cover SZA's from 40°through to 137°. Evidence of kinematic relaxation for quasi-perpendicular shock geometry is also observed throughout this range of SZA. This indicates that when the solar wind conditions are suitable, any location on the Venus bow shock can form a structure in which kinematic relaxation is the dominant energy re-distribution mechanism. Figure 6a shows the estimated Alfvén Mach number plotted against the ratio of the observed to solar minimum model bow shock altitude. The observations are plotted as stars and have been binned according to SZA, which is indicated by the different colors. It shows the tendency for the bow shock to move to a higher altitude as the Mach number falls, which is consistent with previous studies (Russell et al., 1988). However, the effect is more pronounced when $M_A \lesssim 1.4$. This is below the range previously studied by Russell et al. (1988). Above this value the altitude increase is less than a factor of two, but increases to greater than five as $M_A = 1$ is approached. The grouping of the colors of the stars occurs due to the tendency to observe a group of multiple shock crossings across a small time interval. Despite this grouping, it is evident that the SZA does not appear to have a noticeable affect on the abnormal increase in shock altitude as the Mach number decreases. For example, the shocks observed at SZA $\leq 60°$ and SZA $> 120°$ had a similar range of Mach numbers, but show broadly similar increases in altitude. The shocks observed at $100° <$ SZA $\leq 120°$ are split into two groups with lower and higher Mach numbers and their relative increase in altitude is also consistent with the general trend. Figure 6b shows the same data, but plots the Alfvén Mach number against the SZA, with the data binned according to the ratio of the observed to solar minimum model bow shock altitude. This also shows the tendency for the altitude ratio to increase as the Mach number falls. It also highlights that the highest relative altitudes are observed closer to the equator. However, the split either side of the terminator for the $1.5 < A/A_m \leq 2.5$ data (light blue stars) indicates that this feature might be due to the limited observations. In fact, the highly elliptical polar orbit of VEX will bias observations of high altitude bow shock crossings to the polar terminator regions.

To determine if the general trend of increasing relative altitude as the the Mach number falls, is representative of all SZA, the conic section bow shock model (Zhang, Delva, et al., 2008) given by Eq. (1) has been fitted to the data at different Mach numbers. The simple conic section bow shock model used by (Zhang, Delva, et al., 2008) has been chosen as it only requires two parameters (eccentricity ε and terminator altitude L_T) and thus can be estimated using a minimum of two data points. The use of a small number of data points can compromise the accuracy of the estimated model due to the uncertainty in the measurements. However, the objective here is to assess the general trend of the shock location as the Mach number changes, not to determine a high accuracy bow shock model for future predictions. For each model calculation, a minimum of two data points were selected which spanned a Mach number range of 0.02. To ensure that the vertex of the conic section is at the subsolar point, a mixture of dayside and flank shock crossings were selected. The resulting seven Mach numbers chosen for the model (1.07, 1.09, 1.24, 1.34, 1.37, 1.41, 1.55) arise due to the available data and these restrictions on data selection. The full set of data used to determine the models, together with the resulting model parameters and a plot of the relative locations of the models in relation to Venus as included in supplementary material Table S11-S12 and Figure S7 respectively.

$$A_m = \frac{L_T}{1 + \varepsilon \cos(SZA)} \tag{1}$$

The ratio of the Mach number dependent model altitudes to the model altitudes at solar minimum, are plotted in both Figure 6a and b. In Figure 6a the model altitudes are plotted as lines, with the colors corresponding to the SZA bins, i.e. 50° to 130° at 20° intervals. These lines are closely spaced and show the same overall trend, indicating that the relationship between relative bow shock altitude and Mach number is not a function of SZA. In Figure 6b the relative bow shock altitude is indicated by the contour plot, which is consistent with the observations which overlay it. This contour plot indicates that assuming the bow shock can be described by a conic section, as it can be a solar minimum, the relative altitude increase as the solar wind Mach number becomes very small is not significantly affected by the SZA, i.e. similar increases in shock altitude are seen across the observed SZA from 40° through to 140°. At solar minimum Zhang, Delva, et al. (2008) found that the conic section model was a good fit up to a SZA of 117°. For higher SZA a Mach cone was found to fit the data better. This might be the reason that the conic section models start to show a small deviation from the general trend above approximately 120° in Figure 6. However, the deviation is small and the overall trend is still in line with that seen at smaller SZA.

5 Conclusion

Very low Mach number quasi-perpendicular shocks in which the main energy redistribution mechanism is through the kinematic relaxation of non-gyrotropic downstream ion populations have been previously observed in limited studies at Venus (Balikhin et al., 2008), Earth (Pope et al., 2019) and in inter-planetary space (Goncharov et al., 2014; Kajdič et al., 2012; Russell et al., 2009). In this study a thorough survey of Venus Express data during suitable solar wind conditions (i.e. the magnetic cloud phase of an ICME) is conducted to identify the majority of such shocks observed during the entire Venus Express mission. These shocks are then analyzed in terms of the fundamental parameters. The main results of this study can be summarized as:

1. During instances in which Venus interacts with the magnetic cloud phase of an ICME, 92 very low Mach number shock crossings with $M_A = 1.01 - 1.85$ have been identified using Venus Express magnetic field data. To our knowledge these include some of the lowest Mach number shocks to have ever been observed.
2. Within this set of shock crossings, 38 show clear evidence of kinematic relaxation of a non-gyrotropic downstream ion population, in the form coherent oscillations of the magnetic field immediately after the main shock ramp. An additional 19 show some evidence of downstream oscillations or only an overshoot.
3. The shocks showing clear evidence of kinematic relaxation are clustered in a region with $\theta_{B,n} > 50°$ and $M_A < 1.4$. The transition from this region to more quasi-parallel and higher Mach numbers is indicated by the shocks with poten-

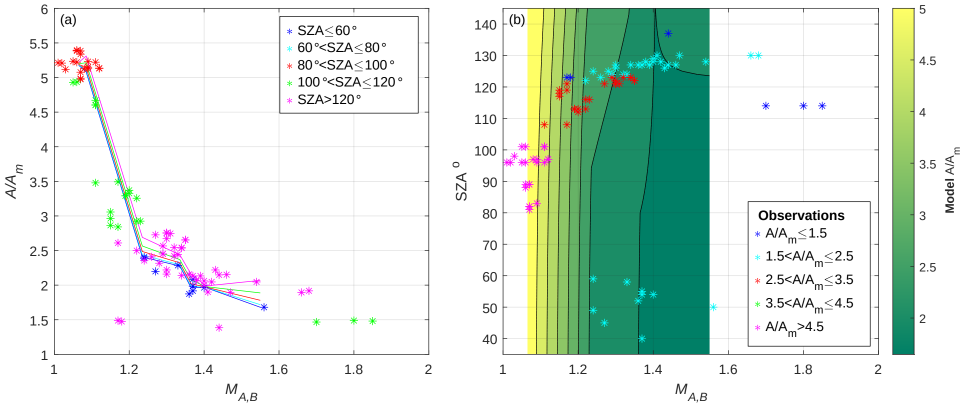

Figure 6. (a) A plot of $M_{A,B}$ against the ratio of the observed to model bow shock altitude A/A_m for all of the very-low Mach number shocks identified for the duration of the Venus Express mission. The observations are plotted as stars and the different colors indicate the different ranges of SZA, which are collected into bins 20° wide. The lines indicate the equivalent Mach number dependent model values at SZA's corresponding to the bins, i.e. 50° to 130° at 20° intervals. (b) A plot of $M_{A,B}$ against the SZA for all of the very-low Mach number shocks identified for the duration of the Venus Express mission. The observations are plotted as stars and different colors indicate the different ratio of the observed to model bow shock altitude A/A_m, which is collected into five bins. These are plotted on top of a contour plot which shows the equivalent Mach number dependent model values.

tially some evidence of downstream oscillations or only an overshoot. Evidence of just an overshoot is likely to be due to the formation of less than one period of downstream oscillations, i.e. a situation in which the oscillations are quickly damped.

4. When Venus Express plasma data was available it generally supports the estimates of fundamental parameters made using the magnetic field alone, in-particular the Alfvén Mach number. Since the proton density is usually very low in magnetic clouds, certain calculations such as the Alfvén velocity, are very sensitive to the inclusion of the effect of heavy ions. In this case the contribution from O^+, most likely occurring as pick-up ions, needed to be included to provide good agreement.
5. The shock crossings which show kinematic relaxation, are observed across a range of solar-zenith-angles from 40°through to 130°. This indicates that it is likely that all locations of the Venus bow shock can form a shock structure in which kinematic relaxation is the dominant energy re-distribution mechanism.
6. The altitude of the observed shocks are generally considerably higher than the Venus model bow shock at solar minimum. The increase in shock altitude is correlated with a reduction in Alfvén Mach number. This is consistent with previous results (Russell et al., 1988). However, the increase is much more pronounced for $M_A \lesssim 1.4$, which is below the range studied by Russell et al. (1988) and does not appear to be affected by the solar zenith angle of the shock location.

Acknowledgments

The author acknowledges the Principal Investigator(s) T. Zhang (OAW, Graz) of the MAG instrument and S. Barabash (IRF, Kiruna, Sweden) of the ASPERA-4 instrument onboard the Venus Express mission for providing datasets in the archive. Datasets of the MAG and ASPERA-4 instrument have been downloaded from the ESA Planetary Science Archive (http://archives.esac.esa.int/psa). The author also acknowledges and appreciates feedback on the manuscript from M. A. Balikhin and support from STFC Consolidator Grant ST/R000697/1.

References

Balikhin, M. A., Zhang, T. L., Gedalin, M., Ganushkina, N. Y., & Pope, S. A. (2008). Venus Express observes a new type of shock with pure kinematic relaxation. *Geophysical Research Letters*, *35*(1).

Barabash, S., Fedorov, A., Sauvaud, J. J., Lundin, R., Russell, C. T., Futaana, Y., ... Bochsler, P. (2007). The loss of ions from Venus through the plasma wake. *Nature*, *450*(7170), 650–653. doi: 10.1038/nature06434

Barabash, S., Sauvaud, J.-A., Gunell, H., Andersson, H., Grigoriev, A., Brinkfeldt, K., ... Bochsler, P. (2007). The Analyser of Space Plasmas and Energetic Atoms (ASPERA-4) for the Venus Express mission. *Planetary and Space Science*, *55*(12), 1772–1792. doi: 10.1016/j.pss.2007.01.014

Burgess, D., Wilkinson, W., & Schwartz, S. (1989). Ion distributions and thermalization at perpendicular and quasi-perpendicular supercritical collisionless shocks. *Journal of Geophysical Research: Space Physics*, *94*(A7), 8783–8792.

Burlaga, L., Sittler, E., Mariani, F., & Schwenn, R. (1981). Magnetic loop behind an interplanetary shock: Voyager, Helios, and IMP 8 observations. *Journal of Geophysical Research: Space Physics*, *86*(A8), 6673–6684.

Burlaga, L. F., & Ogilvie, K. W. (1970). Magnetic and thermal pressures in the solar wind. *Solar Physics*, *15*(1), 61–71. doi: 10.1007/BF00149472

Dimmock, A. P., Alho, M., Kallio, E., Pope, S. A., Zhang, T. L., Kilpua, E., ... Coates, A. J. (2018). The Response of the Venusian Plasma Environment to the Passage of an ICME: Hybrid Simulation Results and Venus Express Observations. *Journal of Geophysical Research: Space Physics*, *123*(5), 3580–3601. doi: 10.1029/2017JA024852

Fedorov, A., Barabash, S., Sauvaud, J.-A., Futaana, Y., Zhang, T. L., Lundin, R., & Ferrier, C. (2011). Measurements of the ion escape rates from Venus for solar minimum. *Journal of Geophysical Research: Space Physics*, *116*(A7), n/a–n/a. doi: 10.1029/2011JA016427

Gedalin, M. (1996). Transmitted ions and ion heating in nearly perpendicular low-mach number shocks. *Journal of Geophysical Research*, *101*, 15569. doi: 10.1029/96JA00924

Gedalin, M. (1997). Ion heating in oblique low-Mach number shocks. *Geophysical Research Letters*, *24*(20), 2511–2514.

Gedalin, M. (2015). Collisionless relaxation of non-gyrotropic downstream ion distributions: dependence on shock parameters. *Journal of Plasma Physics*, *81*(06).

Gedalin, M. (2016). Transmitted, reflected, quasi-reflected, and multiply reflected ions in low-Mach number shocks. *Journal of Geophysical Research: Space Physics*, *121*(11), 10,754–10,767. doi: 10.1002/2016JA023395

Gedalin, M., Friedman, Y., & Balikhin, M. (2015). Collisionless relaxation of downstream ion distributions in low-Mach number shocks. *Physics of Plasmas*, *22*(7), 072301. doi: 10.1063/1.4926452

Goncharov, O., Šafránková, J., Němeček, Z., Přech, L., Pitňa, A., & Zastenker, G. N. (2014). Upstream and downstream wave packets associated with low-Mach number interplanetary shocks. *Geophysical Research Letters*, *41*(22), 8100–8106. doi: 10.1002/2014GL062149

Kajdič, P., Blanco-Cano, X., Aguilar-Rodriguez, E., Russell, C. T., Jian, L. K., & Luhmann, J. G. (2012). Waves upstream and downstream of interplanetary shocks driven by coronal mass ejections. *Journal of Geophysical Research:*

Space Physics, *117*(A6), n/a–n/a. doi: 10.1029/2011JA017381

Kennel, C. F., Edmiston, J. P., & Hada, T. (1985). A quarter century of collisionless shock research. In R. G. Stone & B. T. Tsurutani (Eds.), *Collisionless Shocks in the Heliosphere: A Tutorial Review* (Vol. 34, pp. 1–36). American Geophysical Union Geophysical Monograph Series.

Leamon, R. J. (2002). Properties of magnetic clouds and geomagnetic storms associated with eruption of coronal sigmoids. *Journal of Geophysical Research*, *107*(A9).

Mellott, M. (1985). Subcritical collisionless shock waves. In *Collisionless shocks in the heliosphere: Reviews of current research.*

Ofman, L., Balikhin, M., Russell, C. T., & Gedalin, M. (2009). Collisionless relaxation of ion distributions downstream of laminar quasi-perpendicular shocks. *Journal of Geophysical Research: Space Physics*, *114*(A9).

Ofman, L., & Gedalin, M. (2013). Two-dimensional hybrid simulations of quasi-perpendicular collisionless shock dynamics: Gyrating downstream ion distributions. *Journal of Geophysical Research: Space Physics*, *118*(5), 1828–1836. doi: 10.1029/2012JA018188

Pope, S. A., Gedalin, M., & Balikhin, M. A. (2019). The First Direct Observational Confirmation of Kinematic Collisionless Relaxation in Very Low Mach Number Shocks Near the Earth. *Journal of Geophysical Research: Space Physics*, *124*(3), 1711–1725. doi: 10.1029/2018JA026223

Russell, C. T. (1985). Planetary Bow Shocks. In *Collisionless Shocks in the Heliosphere: Reviews of Current Research* (pp. 109–130). American Geophysical Union. (doi: 10.1029/GM035p0109)

Russell, C. T., Chou, E., Luhmann, J. G., Gazis, P., Brace, L. H., & Hoegy, W. R. (1988). Solar and interplanetary control of the location of the Venus bow shock. *Journal of Geophysical Research*, *93*(A6), 5461. doi: 10.1029/JA093iA06p05461

Russell, C. T., Jian, L. K., Blanco-Cano, X., & Luhmann, J. G. (2009). STEREO observations of upstream and downstream waves at low Mach number shocks. *Geophysical Research Letters*, *36*(3). doi: 10.1029/2008GL036991

Ryu, D., Kang, H., Hallman, E., & Jones, T. W. (2003). Cosmological Shock Waves and Their Role in the Large-Scale Structure of the Universe. *The Astrophysical Journal*, *593*(2), 599–610. doi: 10.1086/376723

Scudder, J. D., Mangeney, A., Lacombe, C., Harvey, C. C., Aggson, T. L., Anderson, R. R., … Russell, C. T. (1986). The resolved layer of a collisionless, high β, supercritical, quasi-perpendicular shock wave: 1. Rankine-Hugoniot geometry, currents, and stationarity. *Journal of Geophysical Research: Space Physics*, *91*(A10), 11019–11052.

Vech, D., Szego, K., Opitz, A., Kajdic, P., Fraenz, M., Kallio, E., & Alho, M. (2015). Space weather effects on the bow shock, the magnetic barrier, and the ion composition boundary at Venus. *Journal of Geophysical Research: Space Physics*, *120*(6), 4613–4627.

Zhang, T. L., Berghofer, G., Magnes, W., Delva, M., Baumjohann, W., Biernat, H., … Motschmann, U. (2007). MAG: The Fluxgate Magnetometer of Venus Express. *ESA Special Publication*, *1295*, 1–10.

Zhang, T. L., Delva, M., Baumjohann, W., Volwerk, M., Russell, C., Barabash, S., … Zambelli, W. (2008). Initial Venus Express magnetic field observations of the Venus bow shock location at solar minimum. *Planetary and Space Science*, *56*(6), 785–789. doi: 10.1016/j.pss.2007.09.012

Zhang, T. L., Pope, S., Balikhin, M., Russell, C. T., Jian, L. K., Volwerk, M., … others (2008). Venus Express observations of an atypically distant bow shock during the passage of an interplanetary coronal mass ejection. *Journal of Geophysical Research: Planets*, *113*(E9).

Zilbersher, D., Gedalin, M., Newbury, J. A., & Russell, C. T. (1998). Direct numerical testing of stationary shock model with low Mach number shock observations. *J. Geophys. Res.*, *103*, 26775. doi: 10.1029/98JA02464

Supporting Information for "A Survey of Venus Shock Crossings Dominated by Kinematic Relaxation"

S. A. Pope[1]

[1]Department of Automatic Control and Systems Engineering, University of Sheffield, Sheffield, UK

Contents of this file

Introduction

The supporting information includes figures showing the profile of the magnetic field magnitude and tables of the key calculated parameters for all of shock crossings identified in this study for time intervals when Venus Express detects the magnetic cloud phase of an interplanetary coronal mass ejection (ICME). A subset of the magnetic field profiles and calculated parameters for the shock crossings is included in the main paper. The shock crossings are grouped into one of six Figures S1 to S6 and Tables S1 to S6 based on the ICME magnetic cloud date. Within each figure and table the shock crossings are grouped into subsets based on the detection of a sequence of shock crossings over a short time interval. Detailed information for each set of crossings is included in the caption for each figure.

The supporting information also includes Tables S7 to S10, which contain the upstream magnetic field and plasma data used to calculate the Alfvén Mach number and plasma β for shock crossings on four of the days studied. Detailed information about the measurement interval used for each set of shock crossings is included in the table captions.

Finally, the supporting information includes Table S11 which contains the list of shock crossings used to determine the bow shock location models at seven different Alfvén Mach numbers and Table S12 which contains the resulting parameters (eccentricity ϵ and terminator altitude L_T) for the conic section model given in Eq. (1). Figure S7 plots the location of these models in relation to the surface of Venus, together with the conic section model previously derived by Zhang et al. (2008) for solar minimum.

$$A_m = \frac{L_T}{1 + \varepsilon \cos(SZA)} \tag{1}$$

References

Zhang, T. L., Delva, M., Baumjohann, W., Volwerk, M., Russell, C., Barabash, S., ... Zambelli, W. (2008). Initial Venus Express magnetic field observations of the Venus bow shock location at solar minimum. *Planetary and Space Science*, *56*(6), 785–789. doi: 10.1016/j.pss.2007.09.012

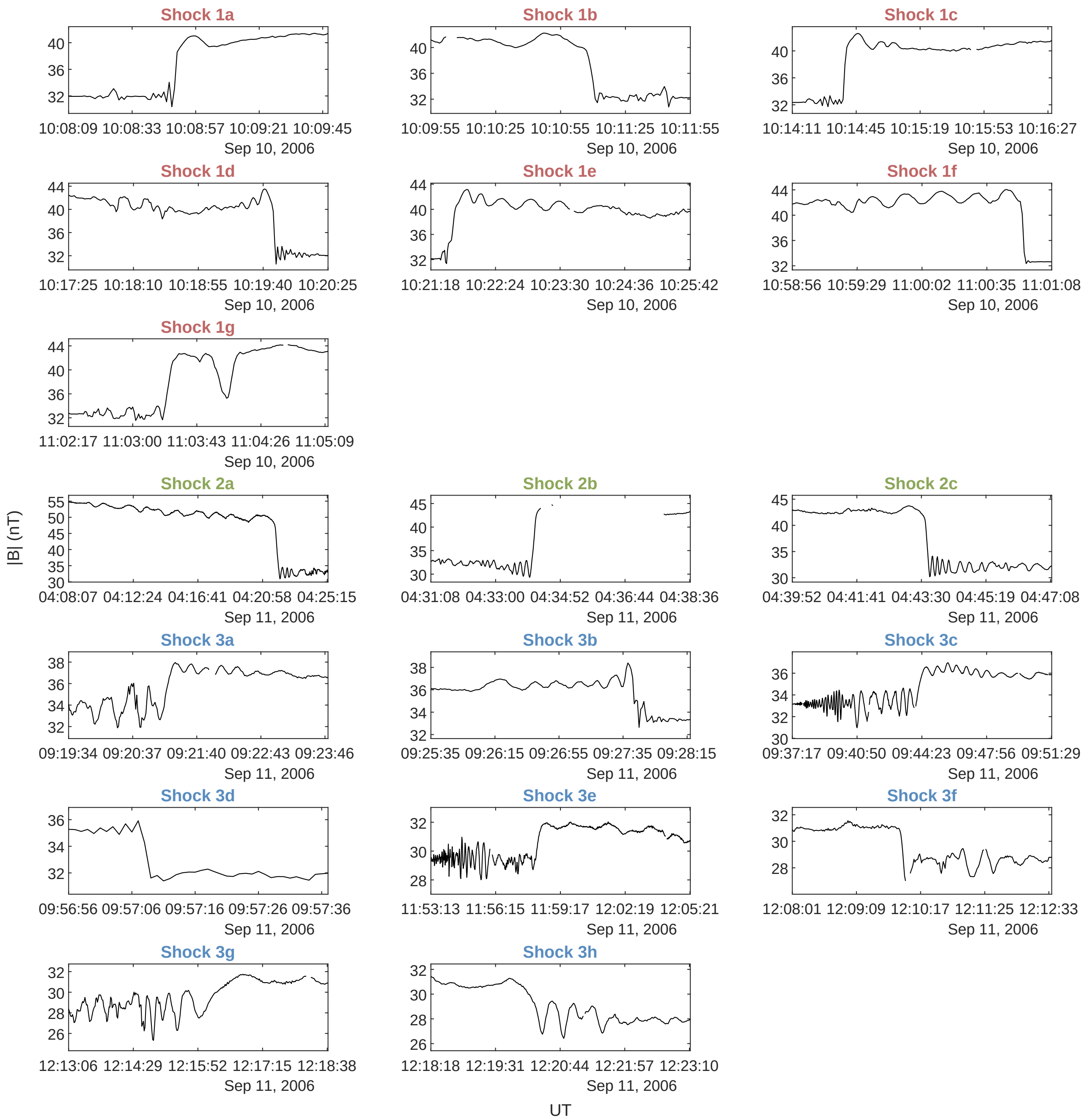

Figure S1. Venus Express magnetic field magnitude plotted for separate intervals showing the individual shock crossings on 10th-11th September 2006 for each of the three colored regions highlighted in Figure 1a of the main paper. The different colored plot titles indicate which of the regions each of the shock crossings belong. For clarity of presentation, the limits of both the time and magnetic field axes are set independently for each panel.

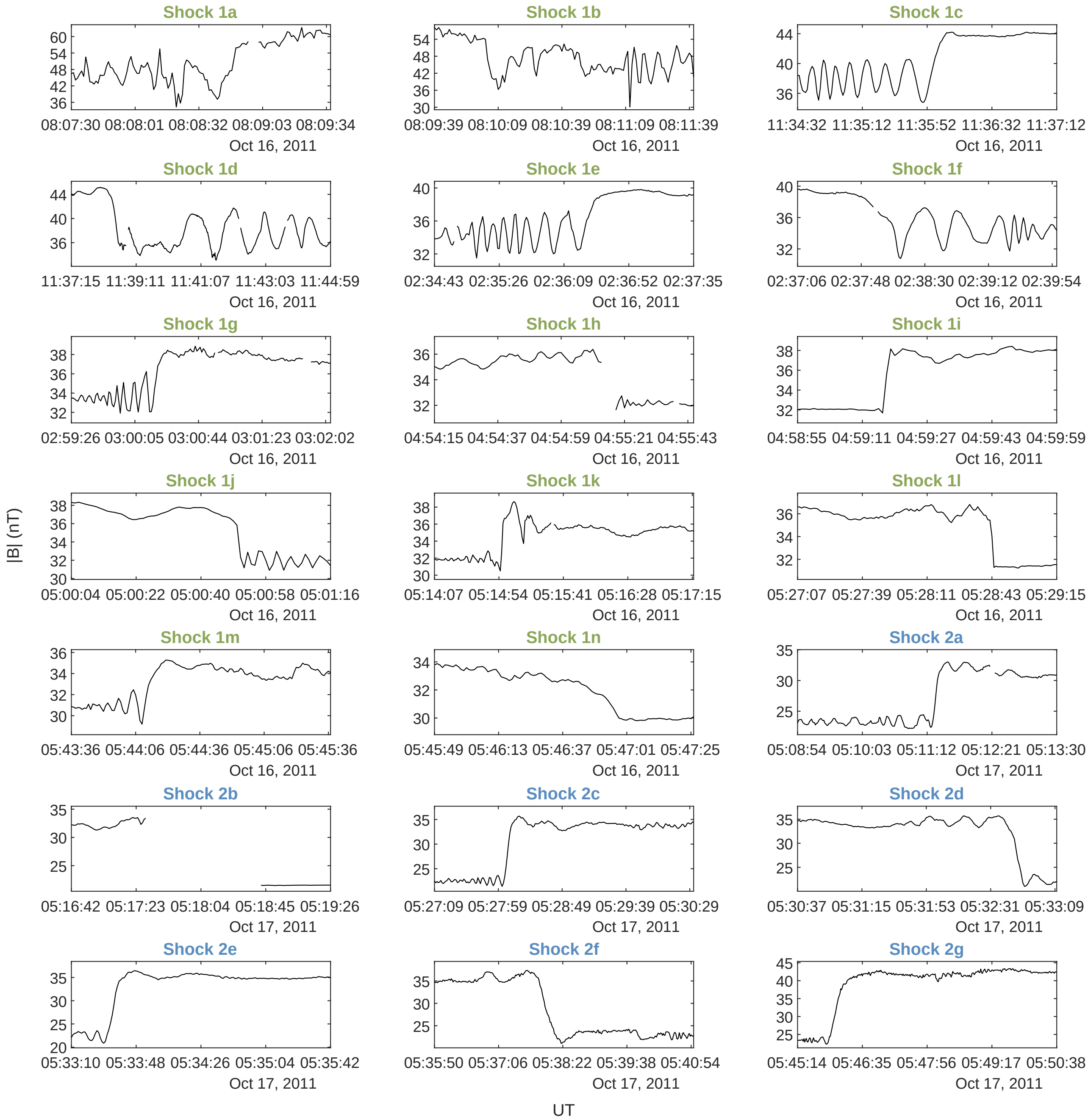

Figure S2. Venus Express magnetic field magnitude plotted for separate intervals showing the individual shock crossings on 16th-17th October 2011 for each of the two regions highlighted in Figure 1b of the main paper. The different colored plot titles indicate which of the regions each of the shock crossings belong. For clarity of presentation, the limits of both the time and magnetic field axes are set independently for each panel.

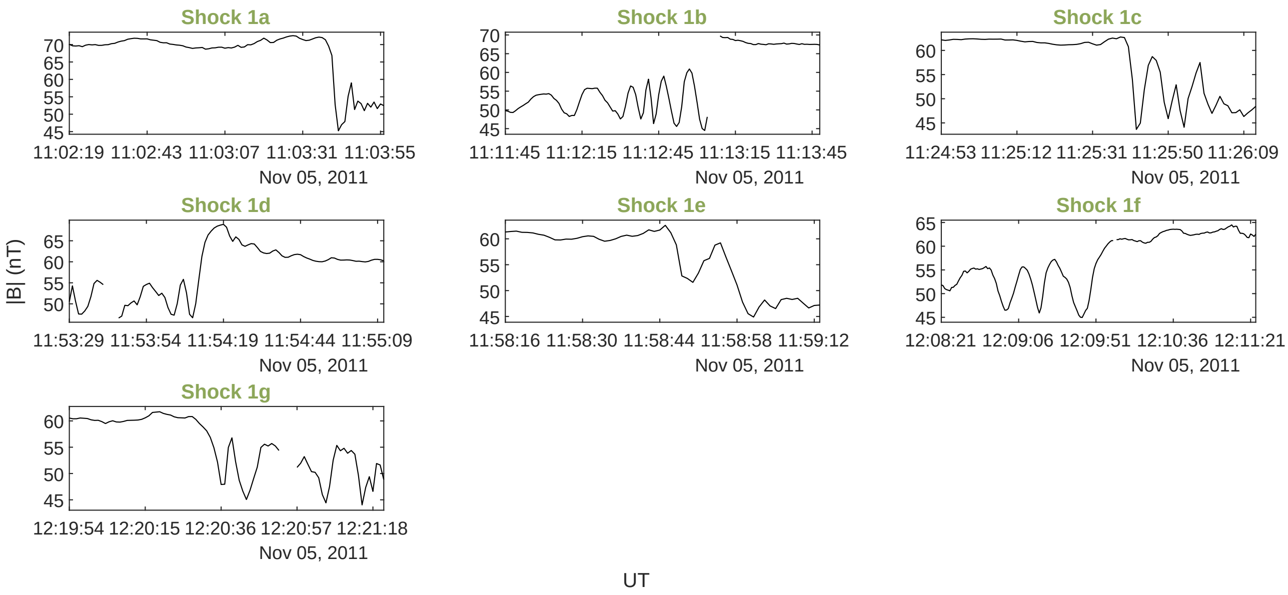

Figure S3. Venus Express magnetic field magnitude plotted for separate intervals showing the individual shock crossings on 5th November 2011 for the green region highlighted in Figure 1c of the main paper. For clarity of presentation, the limits of both the time and magnetic field axes are set independently for each panel.

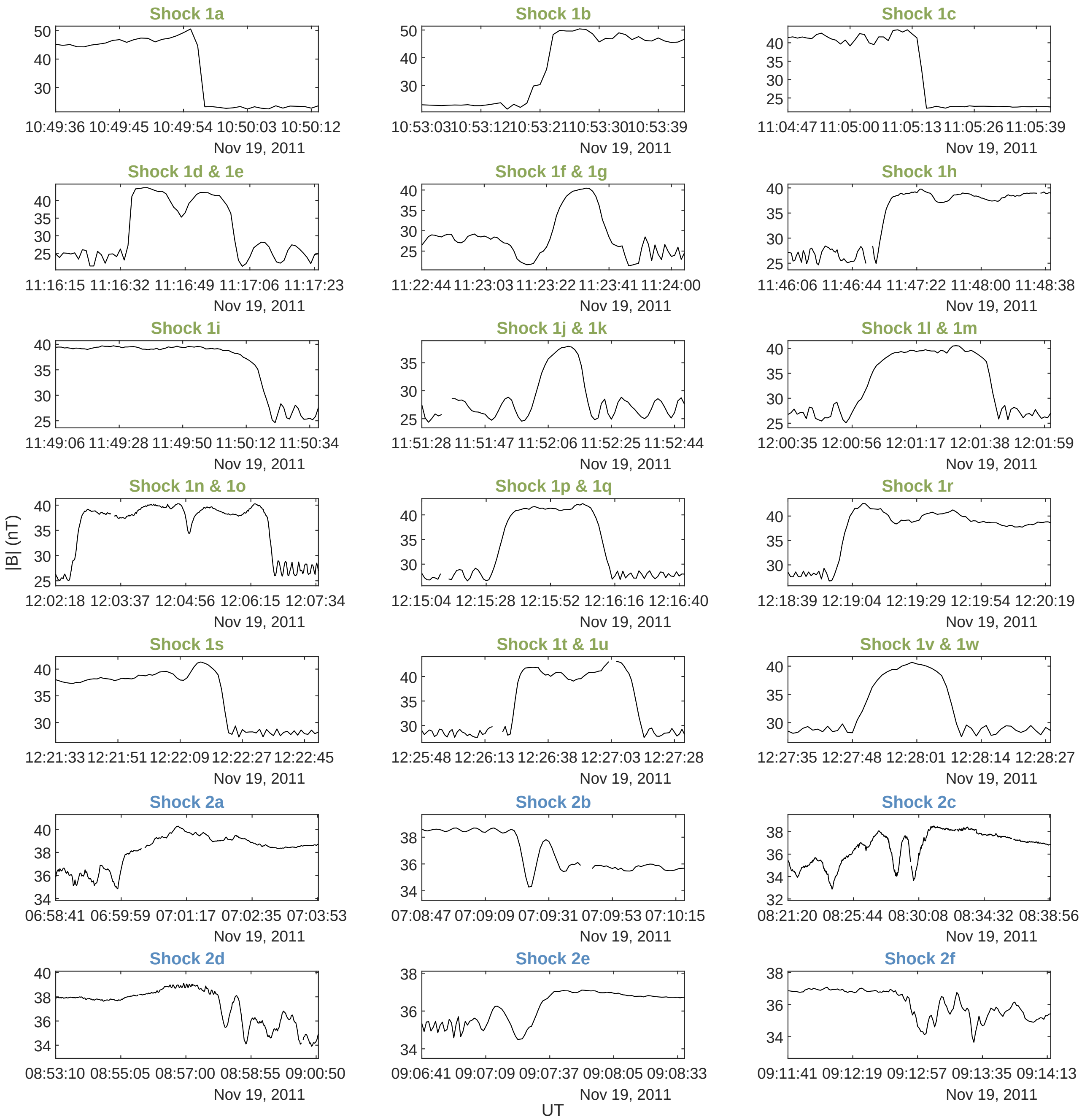

Figure S4. Venus Express magnetic field magnitude plotted for separate intervals showing the individual shock crossings on 19th November 2011 for each of the two colored regions highlighted in Figure 1d of the main paper. The different colored plot titles indicate which of the regions each of the shock crossings belong. For clarity of presentation, the limits of both the time and magnetic field axes are set independently for each panel and two shock crossings are shown on some panels due to the short downstream interval.

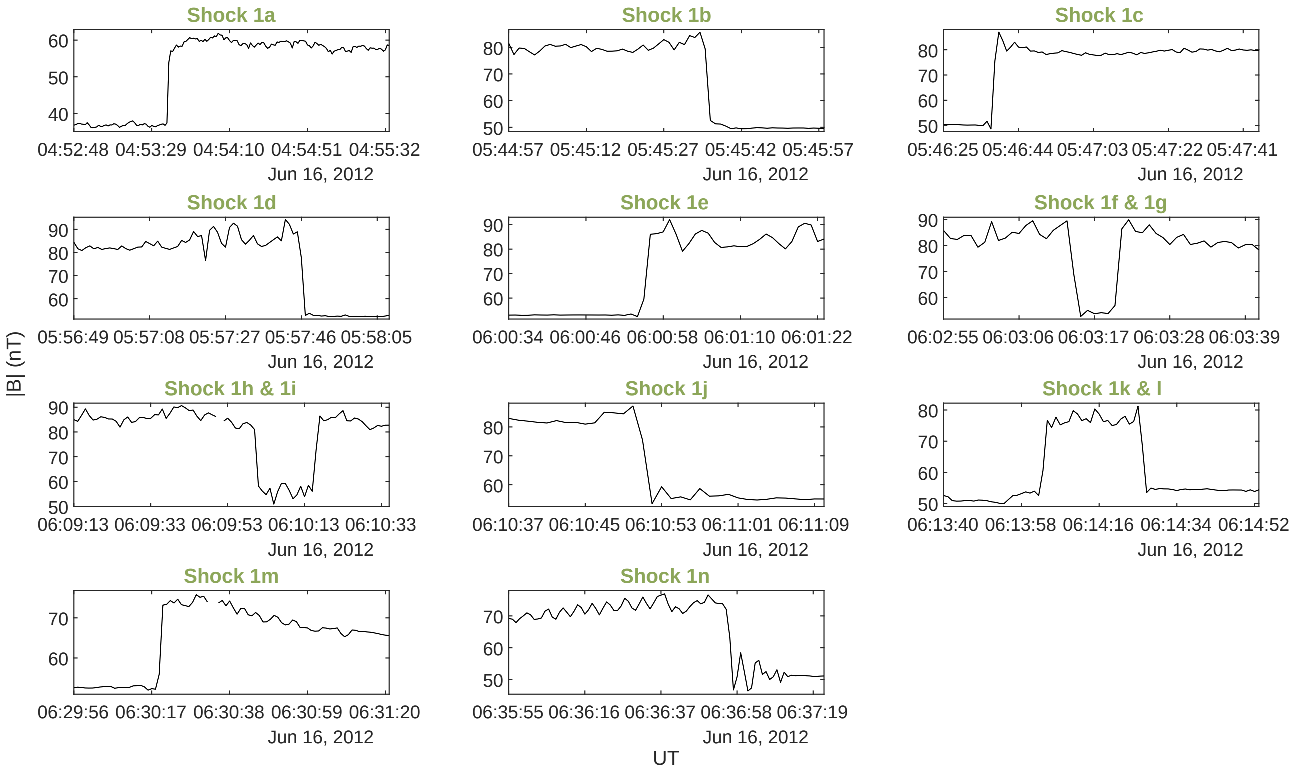

Figure S5. Venus Express magnetic field magnitude plotted for separate intervals showing the individual shock crossings on 16th June 2012 for the green region highlighted in Figure 1e of the main paper. For clarity of presentation, the limits of both the time and magnetic field axes are set independently for each panel and two shock crossings are shown on some panels due to the short upstream/downstream interval.

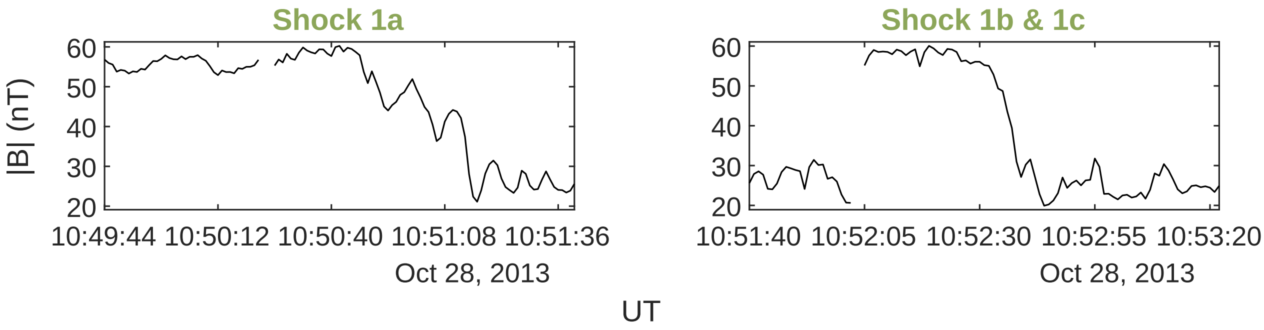

Figure S6. Venus Express magnetic field magnitude plotted for separate intervals showing the individual shock crossings on 28th October 2013 for the green region highlighted in Figure 1f of the main paper. For clarity of presentation, the limits of both the time and magnetic field axes are set independently for each panel and two shock crossings are shown on some panels due to the short downstream interval.

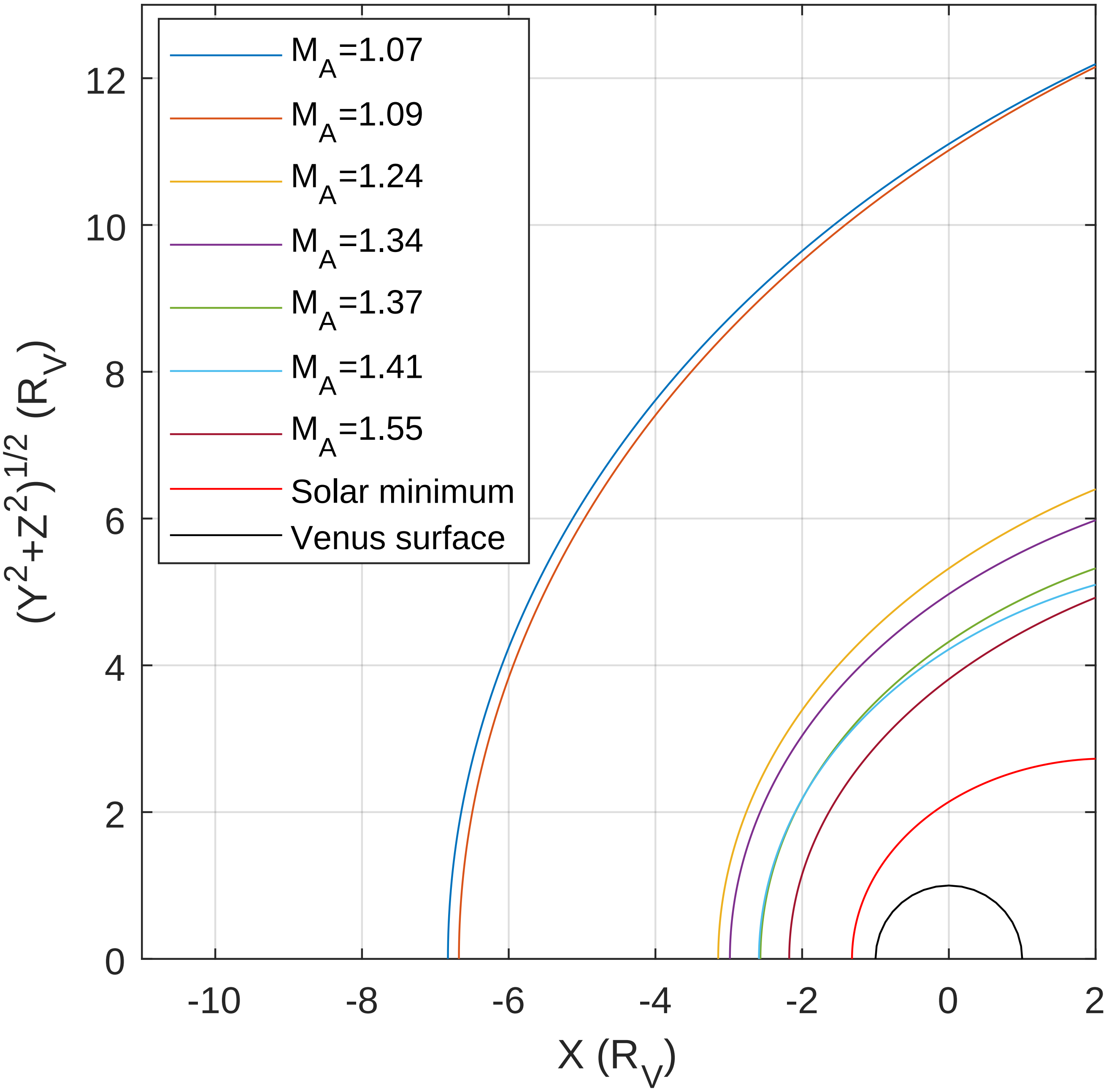

Figure S7. Bow shock location with respect to the surface of Venus for the models determined for seven different Alfvén Mach numbers and the previously determined solar minimum model (Zhang et al., 2008).

Table S1. Magnetic field derived parameters for the three groups of Venus bow shock crossings detected in Venus Express data on the 10-11th September 2006.

Shock	$\theta_{B,n_{mv}}$ (°)	$\theta_{B,n_{cp}}$ (°)	$M_{A,B}$	SZA (°)	A (R_V)	A_m (R_V)
1a	76	70	1.20	112	9.40	2.79
1b	79	79	1.20	113	9.40	2.83
1c	78	63	1.19	113	9.30	2.83
1d	84	83	1.19	113	9.30	2.83
1e	87	70	1.22	113	9.20	2.83
1f	82	80	1.23	116	8.60	2.94
1g	79	78	1.22	116	8.60	2.94
2a	72	71	1.37	40	2.78	1.45
2b	72	76	1.27	45	3.27	1.49
2c	75	51	1.24	49	3.63	1.52
3a	70	49	1.07	81	9.72	1.95
3b	85	63	1.07	82	9.80	1.97
3c	68	64	1.07	82	10.00	1.97
3d	77	53	1.09	83	10.20	1.99
3e	54	47	1.06	88	11.30	2.09
3f	74	54	1.07	89	11.30	2.12
3g	58	55	1.07	89	11.40	2.12
3h	64	64	1.06	89	11.40	2.12

Table S2. Magnetic field derived parameters for the Venus bow shock crossings detected in Venus Express data on the 16-17th October 2011.

Shock	$\theta_{B,n_{mv}}$ (°)	$\theta_{B,n_{cp}}$ (°)	$M_{A,B}$	SZA (°)	A (R_V)	A_m (R_V)
1a	30	26	1.18	123	4.77	3.23
1b	30	21	1.17	123	4.81	3.23
1c	45	52	1.11	108	9.21	2.65
1d	50	42	1.17	108	9.25	2.65
1e	63	63	1.11	101	11.17	2.43
1f	65	67	1.11	101	11.18	2.43
1g	86	62	1.11	101	11.34	2.43
1h	77	58	1.08	97	11.87	2.32
1i	83	42	1.12	97	11.88	2.32
1j	84	70	1.12	97	11.89	2.32
1k	78	43	1.09	97	11.92	2.32
1l	80	64	1.11	96	11.95	2.29
1m	80	66	1.09	96	11.97	2.29
1n	57	11	1.05	96	11.98	2.29
2a	72	71	1.24	59	3.90	1.62
2b	76	68	1.33	58	3.68	1.61
2c	66	65	1.37	55	3.29	1.58
2d	81	72	1.37	54	3.11	1.57
2e	67	68	1.40	54	3.08	1.57
2f	75	68	1.36	52	2.90	1.55
2g	74	69	1.56	50	2.57	1.53

Table S3. Magnetic field derived parameters for the Venus bow crossings detected in Venus Express data on the 5th November 2011.

Shock	$\theta_{B,n_{mv}}$ (°)	$\theta_{B,n_{cp}}$ (°)	$M_{A,B}$	SZA (°)	A (R_V)	A_m (R_V)
1a	58	62	1.26	123	7.79	3.23
1b	15	46	1.22	122	7.97	3.19
1c	45	30	1.17	121	8.21	3.15
1d	61	50	1.17	119	8.70	3.06
1e	13	11	1.15	119	8.77	3.06
1f	47	39	1.15	118	8.95	3.02
1g	54	67	1.15	117	9.11	2.98

Table S4. Magnetic field derived parameters for the Venus bow shock crossings detected in Venus Express data on the 19th November 2011.

Shock	$\theta_{B,n_{mv}}$ (°)	$\theta_{B,n_{cp}}$ (°)	$M_{A,B}$	SZA (°)	A (R_V)	A_m (R_V)
1a	66	65	1.66	130	6.75	3.56
1b	76	60	1.68	130	6.83	3.56
1c	78	83	1.54	128	7.09	3.46
1d	64	58	1.44	127	7.34	3.42
1e	72	68	1.46	127	7.35	3.42
1f	70	62	1.30	126	7.48	3.37
1g	70	56	1.43	126	7.48	3.37
1h	67	63	1.32	124	7.94	3.28
1i	77	71	1.33	124	8.01	3.28
1j	66	60	1.29	124	8.04	3.28
1k	67	62	1.29	124	8.04	3.28
1l	66	68	1.34	123	8.20	3.23
1m	74	70	1.34	123	8.22	3.23
1n	70	71	1.32	123	8.23	3.23
1o	78	70	1.29	123	8.30	3.23
1p	77	75	1.35	122	8.46	3.19
1q	76	73	1.35	122	8.47	3.19
1r	72	73	1.30	122	8.52	3.19
1s	83	73	1.27	121	8.58	3.15
1t	74	73	1.31	121	8.64	3.15
1u	80	74	1.30	121	8.66	3.15
1v	85	77	1.30	121	8.67	3.15
1w	82	79	1.30	121	8.67	3.15
2a	48	41	1.05	101	11.97	2.43
2b	77	55	1.06	101	11.98	2.43
2c	60	39	1.03	98	11.99	2.34
2d	45	33	1.06	96	11.95	2.29
2e	35	2	1.01	96	11.93	2.29
2f	46	20	1.02	96	11.92	2.29

Table S5. Magnetic field derived parameters for the Venus bow shock crossings detected in Venus Express data on the 16th June 2012.

Shock	$\theta_{B,n_{mv}}$ (°)	$\theta_{B,n_{cp}}$ (°)	$M_{A,B}$	SZA (°)	A (R_V)	A_m (R_V)
1a	83	77	1.44	137	5.43	3.92
1b	85	80	1.47	130	6.75	3.56
1c	78	84	1.41	130	6.77	3.56
1d	77	75	1.40	129	7.03	3.51
1e	84	85	1.42	128	7.09	3.46
1f	88	81	1.40	128	7.14	3.46
1g	85	84	1.38	128	7.15	3.46
1h	73	71	1.39	127	7.29	3.42
1i	86	78	1.37	127	7.29	3.42
1j	63	68	1.34	127	7.31	3.42
1k	86	82	1.36	127	7.37	3.42
1l	80	68	1.30	127	7.38	3.42
1m	76	86	1.28	125	7.70	3.32
1n	78	79	1.24	125	7.83	3.32

Table S6. Magnetic field derived parameters for the Venus bow shock crossings detected in Venus Express data on the 28th October 2013.

Shock	$\theta_{B,n_{mv}}$ (°)	$\theta_{B,n_{cp}}$ (°)	$M_{A,B}$	SZA (°)	A (R_V)	A_m (R_V)
1a	61	53	1.70	114	4.20	2.86
1b	54	57	1.85	114	4.24	2.86
1c	62	55	1.80	114	4.26	2.86

Table S7. Measured and calculated upstream parameters for the second and third group of Venus bow shock crossings detected in Venus Express data on 10th-11th September 2006. All values are for protons (unless otherwise indicated), calculated as averages for the upstream u regions (unless otherwise stated) and vectors are in VSO coordinates. The upstream region for the second group is the plasma data with excellent quality flags in-between the first and second shock and for the third group it is the plasma data collected in the magnetic cloud approximately 3 hours after the last shock crossing in this group. * The proton temperature and consequently the calculated β for the second group of shocks is given as a range due to the high variance of the measurements across the time interval of these shocks.

Parameter	Shock group 2	Shock group 3
$\mathbf{B}_u$ (nT)	[-1.6, -20.4, -25.7]	[8.0, 11.3, -15.4]
B_u (nT)	32.9	20.7
$\mathbf{V}_u$ (km/s)	[-349, -1, 62]	[-315, -8, 17]
V_u (km/s)	354	315
n_u (cm^{-3})	2.5	4.1
T_u (eV)	5-14 *	5.8
$V_{a,u}$ (km/s)	457	223
$\beta_{bo,u}$	0.02-0.03	0.08

Table S8. Measured and calculated upstream parameters for shock crossing 2c, 2f and 2g detected in Venus Express data on 16-17th October 2011. All values are for protons (unless otherwise indicated), calculated as averages for the upstream u regions (unless otherwise stated) and vectors are in VSO coordinates.

Parameter	Shock 2c	Shock 2f	Shock 2g
$\mathbf{B}_u$ (nT)	[-0.9, 15.3, -16.4]	[-2.4, -15.2, -18.0]	[-2.5, 12.8, -19.3]
B_u (nT)	22.5	23.7	23.3
$\mathbf{V}_u$ (km/s)	[-414, -77, 119]	[-408, -84, 107]	[-408, -84, 107]
V_u (km/s)	437	430	430
n_u (cm^{-3})	2.2	3.9	3.9
T_u (eV)	28.5	19.7	19.7
$V_{a,u}$ (km/s)	330	263	259
$\beta_{bo,u}$	0.08	0.10	0.10

Table S9. Measured and calculated upstream parameters for shock crossing 2f detected in Venus Express data on 19th November 2011. All values are for protons (unless otherwise indicated) and calculated as averages for the upstream u regions (unless otherwise stated).

Parameter	Shock 2f
B_u (nT)	35.6
V_u (km/s)	617
n_u (cm^{-3})	0.6
T_u (eV)	173
$V_{a,u}$ (km/s)	986
$\beta_{bo,u}$	0.04

Table S11. List of shock crossings used to fit the conic section bow shock model for each Alfvén Mach number considered.

M_A	Shock list
1.07	10-11th September 2006 3a, 3b, 3c, 3e, 3f, 3g, 3h 19th November 2011 2b, 2d
1.09	10-11th September 2006 3d 16-17th October 2011 1f, 1k, 1m
1.24	10-11th September 2006 1f, 2c 16-17th October 2011 2a 16th June 2012 1n
1.34	16-17th October 2011 2b 19th November 2011 1i, 1l, 1m 16th June 2012 1j
1.37	10-11th September 2006 2a 16-17th October 2011 2c, 2d, 2f 16th June 2012 1i, 1k
1.41	17th October 2011 2e 16th June 2012 1c, 1d, 1f
1.55	16-17th October 2011 2g 19th November 2011 1c

Table S12. Parameters for the conic section bow shock model determined for each Alfvén Mach number considered.

M_A	Eccentricity (ε)	Terminator Altitude (L_T)
1.07	0.626	11.1
1.09	0.650	11.0
1.24	0.692	5.32
1.34	0.666	4.97
1.37	0.682	4.32
1.41	0.629	4.22
1.55	0.751	3.81